

DISSERTATION
On
**DEVELOPMENT OF A THERMAL MODEL FOR A TWIN-TUBE
SHOCK ABSORBER: EXPERIMENTAL AND MODELING
APPROACH**

*Submitted in partial fulfillment of the requirement
for the award of degree of*

**Master of Engineering
in
Thermal Engineering**

Submitted By:
Amritveer Singh
Roll No. 801283003

**Under the Guidance of
Dr. Tarun Kumar Bera
*Assistant Professor***



**DEPARTMENT OF MECHANICAL ENGINEERING
THAPAR UNIVERSITY
PATIALA-147004, INDIA
July 2014**

*This Thesis is dedicated to
My Respected Supervisor
Dr. Tarun Kumar Bera*

DECLARATION

I hereby declare that the thesis report entitled “**Development of Thermal Model for Twin-Tube Shock Absorber: Experimental and Modeling Approach**” in the partial fulfillment of the requirements for the award of **Master of Engineering** submitted in **Department of Mechanical (Thermal Engineering) Engineering, Thapar University, Patiala**, is a record of my own work carried out under the supervision and guidance of **DR. TARUN KUMAR BERA, Assistant Professor, Department of Mechanical Engineering, Thapar University**. This matter embodied in this report has not been submitted in part or full to any other university or institute for the award of any degree.



Amritveer Singh

This is to certify that above declaration made by the student concerned is correct to the best of my knowledge and belief.



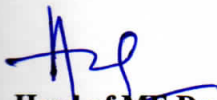
Dr. Tarun Kumar Bera


Assistant Professor

Mechanical Engineering Department

Thapar University, Patiala-147004

Countersigned by:


Head of ME Department
Thapar University
Patiala


Dean of Academic Affairs
Thapar University
Patiala

ACKNOWLEDGEMENT

Words are often less to reveal one's deep regards. With an understanding that work like this can never be the outcome of a single person. I take this opportunity to express my profound sense of gratitude and respect to all those who helped me through the duration of this work.

I would like to express my gratitude and thanks to my supervisor, Dr. Tarun Kumar Bera, Assistant Professor, department of mechanical engineering, Thapar University, Patiala, for his unreserved guidance, constructive suggestions, thought provoking discussions and unabashed inspiration in the nurturing work. It was an honor and privilege to work under him as a student. He also provided the help in technical writing and presentation style and I found his guidance to be extremely valuable.

I am grateful to Dr. Ajay Batish, Professor and Head, Mechanical Engineering Department for providing the facilities for the completion of the work and always being a shelter in the odd days.

I am also thankful to the faculty in mechanical workshop who devoted their valuable time for the successful completion of experimental work of this dissertation.

Finally, I am grateful to my parents, without their encouragement, patience and moral support, it would not have been possible for me to complete my thesis.

Amritveer Singh

Amritveer Singh

Reg. No. 801283003

ABSTRACT

The automotive suspensions play a crucial role in vehicle safety and driving comfort. Their function is to damp the vibrations produced in the spring due to external excitation. As the shock absorber is compressed and extended, hydraulic fluid starts to flow between the upper chamber and lower chamber through the piston orifice. Piston orifice restricts the flow of hydraulic fluid through it, thereby providing the required damping action. Therefore, the geometrical configuration of piston orifice decides the amount of damping. Further there is a rise in the temperature of hydraulic fluid. This heat needs to be dissipated to the surrounding; otherwise the performance of shock absorber gets reduced.

Keeping in view the role of heat generation and dissipation, the aim of this dissertation is to develop a thermal model for the twin-tube hydraulic shock absorber using bond graph method. In this thesis, experiment is conducted on a rear shock absorber of Tata Innova. Temperature at the upper and lower part of the shock absorber is measured with the k-type thermocouples. Bond graph model for the twin-tube hydraulic shock absorber is developed. Simulation results are compared with the experimental results to validate the model. Both the experimental and simulation results show that the volume flow rate of hydraulic fluid is more in the upper chamber as compared to that in the lower chamber. Temperature of hydraulic fluid in the upper and lower chamber is calculated by taking enthalpy as flow variable in the bond graph. Temperature rises linearly with respect to time. There is a saturation of temperature after some time. At this point, the surface temperature and hydraulic fluid temperature become equal and shock acts as a single entity transferring heat to the surroundings. This point marks the point of maximum heat transfer to the surroundings. For any shock absorber, it is always desirable to achieve the saturation point as early as possible. The bond graph model developed in this thesis work may be used by the manufacturers to know the hydraulic and thermal performance of their product. Further, it will help the manufacturers in deciding the size and number of piston orifices which is deciding factor for the comfort level of the vehicle.

Keywords: Twin-tube shock absorber, Temperature, Volume flow rate, Pressure development, Bond graph, Experiment.

LIST OF ABBREVIATIONS

C	Capacitance
De	Effort Detector
Df	Flow Detector
DSSA	Displacement Sensitive Shock Absorber
GY	Gyrator
I	Inertance
MSE	Modulated Sources of Effort
MSF	Modulated Sources of Flow
MTF	Modulated Transformer
R	Resistance
Se	Source of Effort
Sf	Source of Flow
TF	Transformer

NOMENCLATURE

A	Area
A_v	Area of piston orifice
C_{di}	Coefficient of discharge for inlet flow
C_{do}	Coefficient of discharge for outlet flow
C_p	Specific heat of hydraulic fluid
f	Friction loss
G	Gibbs free energy
h	Enthalpy
H	Convective heat transfer coefficient
i	Current
k	Thermal conductivity
L	Length
\dot{m}	Mass flow rate of hydraulic fluid
P	Pressure
\dot{q}	Rate of heat transfer
\dot{Q}	Volume flow rate of hydraulic fluid
r_1	Inner radius of inner cylinder
r_2	Outer radius of inner cylinder
r_3	Inner radius of outer cylinder
r_4	Outer radius of outer cylinder
S	Entropy
t	Time
T	Temperature
U	Internal energy
v	Piston Speed
V	Volume
\dot{W}	Rate of work done
ω	Frequency
μ	Dynamic viscosity

μ_1	Second viscosity coefficient
β	Bulk modulus of elasticity
δ	Kronecker delta
ρ	Average density of hydraulic fluid
σ	Stress acting on the fluid element

SUBSCRIPT

a	Anisotropic
c	Chamber
lc	Lower Chamber
p	Piston
po	Piston Orifice
r	Piston Rod
r_1	Inner radius of inner cylinder
r_2	Outer radius of inner cylinder
r_3	Inner radius of outer cylinder
r_4	Outer radius of outer cylinder
uc	Upper Chamber
u-l	Upper chamber to Lower Chamber
uc-p	Upper Chamber to Piston
uc-r	Upper Chamber to Piston Rod

LIST OF FIGURES

Figure No.	Caption of Figure	Page No.
1.1	Diagram of a twin-tube shock absorber	4
1.2	Diagram of the single-tube shock absorber	7
3.1	Bond Graph for Transformer	23
3.2	Bond Graph for Gyrator	23
3.3	(a) Electrical circuit having voltage source and resistor	26
	(b) Causalled Bond Graph for the circuit	26
3.4	Causality of source of effort	27
3.5	Causality of source of flow	27
3.6	Integral Causality of inertial element	27
3.7	Integral Causality of compliant element	28
3.8	(a) Electrical circuit having source of effort	28
	(b) Causality of resistive element when it receives effort	28
3.9	(a) Electrical circuit having source of flow	29
	(b) Causality of resistive element when it receives flow	29
3.10	Causality of transformer element when flow is from left to right	29
3.11	Causality of transformer element when flow is from right to left	29
3.12	Causality of gyrator element	29
3.13	Causality of 0-junction	30
3.14	Causality of 1-junction	30
3.15	Differential causality of I element	31
3.16	Differential causality of C element	31
3.17	Control volume with thermally conducting wall containing gas	31
3.18	A basic thermal C-field	32
3.19	Modified Thermal C-field	33
3.20	Basic Bond Graph Model for Shock Absorber	43
3.21	Thermal bond graph model for twin-tube shock absorber	44

3.22	Variation of Input Force with Time	46
3.23	Variation of Piston Displacement with Time	47
3.24	Variation of Pressure Developed in Upper and Lower Chamber at	49
	(a) 1" stroke length	49
	(b) 2" stroke length	49
	(c) 3" stroke length	49
	(d) 4" stroke length	49
3.25	Volume flow into and out of upper chamber of shock absorber at	51
	(a) 1" stroke length	51
	(b) 2" stroke length	51
	(c) 3" stroke length	51
	(d) 4" stroke length	51
3.26	Volume flow into and out of lower chamber of shock absorber at	52
	(a) 1" stroke length	52
	(b) 2" stroke length	52
	(c) 3" stroke length	52
	(d) 4" stroke length	52
3.27	Variation of Oil Temperature for Upper chamber and Lower chamber at	54
	(a) 1" stroke length	54
	(b) 2" stroke length	54
	(c) 3" stroke length	54
	(d) 4" stroke length	54
3.28	Comparison between the Oil Temperature and surface temperature for Upper chamber and Lower chamber at	55–56
	(a) 1" stroke length	55
	(b) 2" stroke length	55
	(c) 3" stroke length	56
	(d) 4" stroke length	56
4.1	Twin-Tube shock absorber fixed on the slotting machine for temperature measurement	57

4.2	Twin-Tube shock absorber fixed on a dynamometer for force measurement	58
4.3	4-Component Dynamometer (Type 9272)	59
4.4	Multi charge Amplifier	60
4.5	K-type Wire Thermocouple with Display Unit	61
4.6	Slotting Machine	63
4.7	Variation of Temperature for the experimental and simulation results at	65–66
	(a) 1" stroke length	65
	(b) 2" stroke length	65
	(c) 3"stroke length	66
	(d) 4" stroke length	66

LIST OF TABLES

Table No.	Caption of Table	Page No.
3.1	Power Variables in Different Energy Domains	20
3.2	Bond Graph Elements	25–26
3.3	Parameter values for the hydraulic and thermal model of twin-tube shock absorber	45–46
4.1	Shock Absorber Dimensions	62

TABLE OF CONTENTS

DECLARATION	ii
ACKNOWLEDGEMENT	iii
ABSTRACT	iv
LIST OF ABBREVIATION	v
NOMENCLATURE	vi
SUBSCRIPT	viii
LIST OF FIGURES	ix
LIST OF TABLES	xii
CHAPTER 1: INTRODUCTION	1–10
1.1. Background and Motivation	1
1.2. Vehicle Suspension System	2
1.3. Shock Absorber	3
1.3.1. Types of Shock Absorbers	4
1.4. Comparison between the Mono-Tube and Twin-Tube Shock absorber	8
1.5. Contribution of the Thesis	9
1.6. Organization of the Thesis	9
CHAPTER 2: LITERATURE REVIEW	11–18
2.1. Introduction	11
2.2. Applications of Bond graph Modeling	11
2.3. Shock Absorber Modeling	12
2.4. Literature Gap	18
2.5. Objective of the Present Work	18
CHAPTER 3: DEVELOPMENT OF THERMAL MODEL OF HYDRAULIC SHOCK ABSORBER	19–56
3.1. Introduction	19

3.2. Bond Graph	19
3.2.1. Elements of Bond Graph	21
3.2.2. Junctions	24
3.2.3. Causality	26
3.2.4. Bond Graph Applied to Thermal System	31
3.3. Theoretical Model of Shock Absorber	34
3.3.1. Energy equation for the Upper Chamber and Lower Chamber Oil	34
3.4. Thermal Model for Bond Graph Analysis	39
3.4.1. Basic Model of Shock Absorber	39
3.4.2. Thermal Model	43
3.4.3. Thermal Model with Heat losses	45
3.5. Parameter values and Simulation Results	45
3.5.1. Variation of Input Force with Time	46
3.5.2. Variation of Piston Displacement with Time	47
3.5.3. Variation of Pressure Developed in Upper and Lower Chamber at different stroke lengths with time	48
3.5.4. Volume flow rate for the Upper chamber and Lower chamber	50
3.5.5. Variation of Oil Temperature for Upper chamber and Lower chamber with Time	53
3.5.6. Comparison between Oil Temperature and surface temperature for Upper lower chamber	55
CHAPTER 4: EXPERIMENT STUDY	57–66
4.1. Introduction	57
4.2. Experimental Setup	57
4.2.1. 4-Component Dynamometer (Type 9272)	59
4.2.2. Multichannel Charge Amplifier for Multi component Force Measurement	60
4.2.3. K-Type Thermocouple with Display Unit	60
4.2.4. Twin-Tube Shock Absorber	62
4.2.5. Slotting Machine	63
4.3. Comparison of Simulation and Experimental Temperature Profiles	64

CHAPTER 5: CONCLUSIONS	67–68
5.1. Conclusion	67
5.2. Scope for Future Work	68
REFERENCES	69
CURRICULUM VITAE	72

Irregularities present in the road surface often lead to the longitudinal, vertical and transversal vibrations in the vehicle, which results in the loss of comfort and control over the vehicle [1]. Further, the effectiveness of the braking system and steering system is also reduced due to these vibrations. Thus, an effective suspension system plays a crucial role in the vehicle safety and comfort to the passengers. Shock absorber is one of the parts of the suspension system and its function is to dampen the vibrations produced due to roughness in the road surface. Based on the requirement, different types of shock absorbers are available in the market. The so-called twin-tube shock absorbers are used in almost all the four wheelers whereas mono-tube shock absorbers are used in the two wheelers. Further, the modification of twin-tube shock absorber known as Displacement sensitive shock absorber (DSSA) are known for the high level of comfort and are used in the luxury cars.

The automotive suspension plays a crucial role in vehicle safety and driving comfort. Even if isolation from road vibration is definitely a very important, maintaining the contact between road surface and vehicle wheels is also necessary as the control and stability of the vehicle rely totally upon it [2]. The main components of suspension are dampers and springs, both positioned between the sprung mass (vehicle body) and the unsprung mass (wheel). Although, the name shock absorber is commonly used for dampers, in reality vehicle shocks are absorbed by the deflection of the wheels and springs. The principal purpose of dampers is to dissipate energy. As the damper is compressed and extended, mechanical energy is converted into heat, damping the vehicle oscillations and improving road adhesion.

1.1 BACKGROUND AND MOTIVATION

Shocks absorbers are used to damp oscillations by absorbing the energy contained in the springs or torsion bars when the wheels of an automobile move up and down. There are many types of shock absorbers. Earlier mono tube shock absorbers were used in cars and heavy vehicles. Now days, most cars are coming with gas filled twin tube shock absorbers as they provide a better performance characteristics thereby, increasing the comfort level of rider to a great extent. Moreover the wheel-load variations which are dynamic in nature are reduced to a great extent and the wheels of the vehicle are prevented from elating off the road and thus adding to the more

accurate steering and braking. The shock absorber converts the kinetic energy of up and down motion of vehicle into thermal energy and this heat needs to be dissipated to the atmosphere. This is the working principle of shock absorbers. If the generated heat is not dissipated properly to the atmosphere, it is going to adversely affect the properties of working fluid *i.e.*, viscosity of the fluid will decrease which further led to trapping off air in the oil. This will decrease the performance of shock absorber. So, it is important to know the thermal behavior of the shock absorber *i.e.*, temperature development in the upper and lower chamber, volume flow rate of oil through the piston orifice *etc.* The above mentioned reasons lead to motivation to develop a thermal model for twin tube shock absorber which could help the manufacturers to know about the thermal behavior of the shock absorber and accordingly they can make the necessary changes in the existing shock absorbers.

1.2 VEHICLE SUSPENSION SYSTEM

Spring, shock absorber, anti-sway bar are main components of any vehicle suspension system. The function of vehicle suspension system is to isolate the vehicle from the vibrations, noise and bumps caused due to irregularities on the road surface which further lead to efficient control over the steering and braking system of the vehicle. In a nutshell, an efficient suspension system serves to provide comfort to the passenger. When the wheels of the vehicle hits an obstruction, the spring part of the suspension system starts to vibrate and now it is the function of shock absorber to damp out these vibrations. The suspension system is designed in such a way that a good compromise between the ride comfort, vehicle handling and load carrying capacity could be done.

The springs used in suspension system are of many type *i.e.*, leaf springs, coil springs, torsion bars. Leaf springs are used at the rear suspension of heavy transport vehicles. Light coil springs are used in modern commercial vehicles. Likewise, there are many type of shock absorbers used in the vehicle suspension system. Twin-tube shock absorbers are most prevalent these days. Earlier, the cars were mostly having simple twin-tube shock absorbers. Now days, gas filled twin-tube configuration is in common use in the new models of almost every car. Further the displacement sensitive twin-tube shock absorbers are used in expensive luxury cars where the human comfort is the main factor considered while manufacturing. Another type of

shock absorbers which became obsolete these days is mono-tube shock absorber. These days, mono-tube shock absorbers are used on bikes and scooters.

1.3 SHOCK ABSORBER

Basically, a shock absorber is a piston cylinder arrangement in which there is a motion of oil between the upper and lower chamber through the piston valve. The upper part of the shock absorber is attached to the vehicle chassis which acts as sprung mass and the lower end of the shock absorber is connected to the wheels of the vehicle which acts as unsprung mass. Roughness on the road surface acts as external disturbing force which puts the spring of the suspension system in the vibrating mode. Now, there is a need to damp out these vibrations to achieve the required comfort level. The job of damping out these vibrations is performed by the shock absorber.

There are two cycles in the working of shock absorber. These are compression cycle and rebound cycle. When the wheels of the vehicle hit an obstruction on the road, there will be a vibration in the spring of the suspension system. Shock absorber performs the job of damping the vibrations. During the compression, the piston moves down. Due to this, the pressure in the lower chamber rises and oil starts to flow into the upper chamber through the piston valve. The piston valve offers resistance to the flow of oil through it. It is due to this resistance, the damping of vibrations of spring takes place. The amount of this resistive force depends on the number of piston valves, geometrical construction and the size of piston valve.

During the rebound stroke of the piston, it moves upwards inside the cylinder. There is pressure rise in the upper chamber of the shock absorber. This leads to the flow of oil from the upper chamber to the lower chamber through the piston valve. Normally, the resistive force offered by the piston valve to the flow of oil through it is more for the rebound stroke as compared to the compression stroke. This difference in the resistive forces for the rebound and compression strokes is due to the geometrical configuration of the piston valve. There is conversion of kinetic energy of vibrations to the heat energy when the shock absorber performs its function. This heat is transmitted to the atmosphere.

1.3.1 Types of Shock Absorbers

Based on the number of the tubes, shock absorbers can be classified as twin-tube and mono-tube shock absorbers. Twin-tube shock absorbers are used in almost all the four wheelers whereas mono-tube shock absorbers are used in bikes and scooters. Further, there are various types of twin-tube shock absorbers used now days.

- **Twin-Tube Shock Absorber**

Twin-tube shock absorbers are of many types. The simple twin-tube shock absorber is shown in Fig. 1.1. There are two tubes in this shock absorber. The inner tube is known as the pressure tube. The outer tube which contains pressurized air also contains oil.

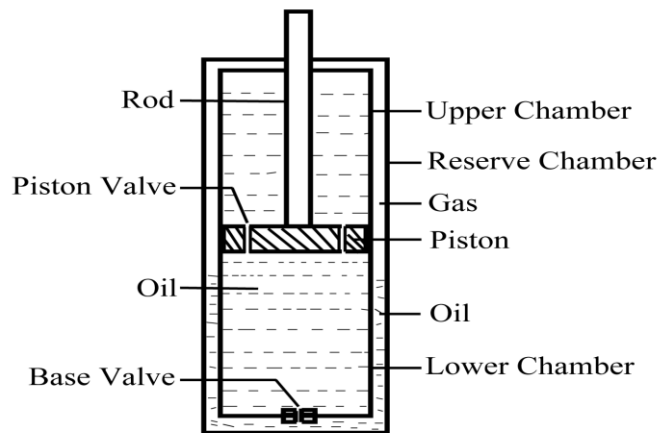


Fig. 1.1 Diagram of a twin-tube shock absorber

The upper part of the shock absorber is called upper chamber and the lower part is known as lower chamber. The control volume representing the upper chamber and lower chamber changes according to the piston displacement. During the compression stroke, the piston moves downwards. Oil starts to flow from lower chamber to upper chamber through the piston valve and the volume of oil equivalent to volume of piston rod enters the reserve chamber by a base valve. The air in the reserve chamber gets compressed. This compressed air provides extra effort to the shock absorber during the rebound stroke. There is a rod guide at the upper part of the shock absorber whose function is to keep the piston rod parallel to the pressure tube in a straight line and this leads to the free movement of the piston inside the cylinder with negligible contact friction between the piston and cylinder body. The seal is provided at the top

part where piston rod is inserted into the cylinder and its function is to prevent the leakage of hydraulic oil and to keep the contaminations out.

Higher potential control levels are needed for the larger shock absorbers with larger piston area and piston displacement. The operating pressure and temperature is lower for the shock absorbers with larger piston area. Higher damping is achieved with this type of design. Further the damping affect produced by the damper also depends upon the size of piston valve and number of piston valves. Following are the various types of twin-tube shock absorbers:

1. Basic twin-tube: It is also called double-tube shock absorber. This device has two concentric cylindrical tubes; an inner tube is called the working tube whereas an outer tube is known as reserve tube. There is a base valve or compression valve at the bottom part of an inner tube. There are small orifices in the piston known as piston valves. As soon as the piston is enforced up or down due to obstructions on the road surface, the hydraulic fluid starts to flow among upper and lower chamber through the piston valve and between lower chamber and reserve chamber through the base valve. Piston valve and base valve resist the flow of fluids between these chambers. So, there is conversion of kinetic energy into heat energy. This heat is dissipated to the atmosphere and the performance of any shock absorber depends on its ability to dissipate this heat in the minimum possible time.

2. Twin-tube gas charged: It is also called gas cell double-tube shock absorber. This is the advanced version of basic twin-tube shock absorber developed mainly to increase the ride comfort and better rebound stroke of the shock absorber. Its overall construction is very much comparable to the basic twin-tube type construction; the only addition in this is that a low pressure nitrogen gas is charged into the reserve tube. The advantage of this addition is a remarkable decline in aeration of hydraulic fluid. In basic twin-tube configuration, there is problem of leakage of hydraulic fluid by aeration or foaming which occurs due overheating of hydraulic fluid. Most of the present day modern vehicles are the gas filled twin-tube shock absorbers.

3. Position sensitive damping: This type of shock absorber is often abbreviated as PSD. This type of design is another advancement of the twin-tube type shock absorber. This design is similar to the gas filled twin-tube shock absorbers but the only addition is of two grooves at the

middle portion of the shock absorber. This modification is aimed at increasing ride comfort of luxury cars even when a car encounters a bump of very small size (bumps at traffic lights, railways stoppers) where a normal gas filled shock absorber ceased to work due to very small external excitation force required for pushing the shock absorber. This design allows the hydraulic fluid to pass through the two grooves with less resistance when the car encounters bumps of small size. In this way, an increased comfort to the rider is achieved with the position sensitive twin-tube shock absorber.

4. Acceleration sensitive damping: The next important stage in shock absorber progress is ASD *i.e.*, the acceleration sensitive shock absorber which is designed to take care of individual bumps and not just to the circumstantial alteration from rough to smooth conditions for bumps of very small size as is achieved by the position sensitive shock absorbers. The modifications in design of base are done in order to make the shock absorber acceleration sensitive. This technology has provided a great control over the steering and braking and increased comfort to the rider. Further there is reduced pitch while braking and reduced rolling of vehicle while turning. This design is however, not coming with the present vehicles but one can have this type shock absorber installed later on. Only a few manufacturers are manufacturing this type of shock absorbers.

5. Coil over: These are twin-tube gas charged shock absorbers with a metal coil. Though these are common on motorcycle and scooter rear suspensions, coil over shocks are uncommon in original equipment designs for vehicles. Coil over shocks for cars have been considered specialty items for high performance and racing applications where they allow for significant reductions in overall vehicle height and though high-quality aftermarket options with wide sturdy springs may provide improvements in vehicle performance, there is dispute over whether or not most aftermarket coil over shocks confer any material benefits to most drivers and may in fact reduce performance over original equipment installations.

- **Mono-Tube Shock Absorber**

The construction of a mono-tube shock absorber is shown in Fig. 1.2. Unlike twin-tube shock absorbers, there is only one tube called pressure tube in this type of shock absorber. Another difference between the twin-tube and mono-tube shock absorber is that in the twin-tube shock absorber, the rod part of the shock absorber is attached to the vehicle chassis and the bottom part

to axle whereas, in mono-tube shock absorber, the rod part is connected to the axle and other part of shock absorber is connected to the chassis. Further, two pistons are present inside the pressure tube. Piston which is connected to the rod is known as working piston and the other piston is known as dividing piston. The function of dividing piston is to act as a separating wall between the hydraulic fluid in the working chamber and gas in the equalizing chamber. The working piston has two valves called piston valves. The length of the pressure tube in case of mono-tube shock absorber is large as compared to that of twin-tube shock absorber to have capacity for dead length. Nitrogen gas at a pressure of 360 psi is filled into the equalization chamber. This high pressure gas serves to support a part of vehicle's weight. Oil is contained in the working chamber below the dividing piston. When the vehicle hits an obstruction, the piston rod starts to reciprocate inside the working chamber which leads to the up and down movement of dividing piston.

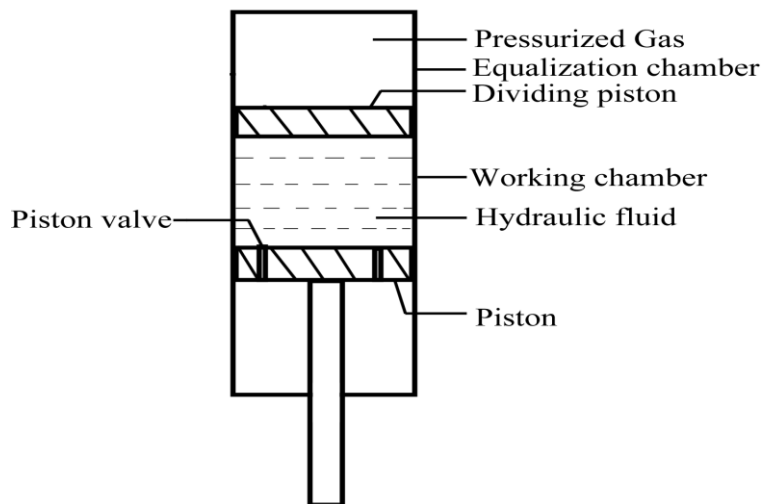


Fig. 1.2 Diagram of the single-tube shock absorber

As the wheels of the vehicle get the external excitation-force from the bumps in the road, the hydraulic fluid starts to flow from the upper part of the working chamber into the lower part via piston valve. Due to high pressure of gas in equalization chamber, there will be a return stroke which forces hydraulic fluid to flow from the lower part to upper part of the working chamber through the piston valve. Damping action is produced when the piston valve offers resistance to the flow of hydraulic fluid through it. This type of shock absorber is not used in passenger cars because of large length of tube. This type of shockers can be fitted in either position *i.e.*, piston rod end can be connected to axle as well as to the chassis of the vehicle. The

entire shock absorber action vests in the geometrical construction of the piston and piston valves for this type of shock absorber.

1.4 COMPARISON BETWEEN THE MONO-TUBE AND TWIN-TUBE SHOCK ABSORBERS

Characteristic features of twin-tube shock absorber are as follows:

- Gas pressure used is comparatively low (30–100 psi).
- Manufacturing cost is low.
- Twin tube shock absorber responds better and more quickly to altering weight and road conditions as compared to mono-tube shock absorbers.
- Increased control over the steering and braking system along with increased comfort level.
- It can be mounted only in one particular direction.
- Heat dissipation is low.

Characteristic feature of mono-tube shock absorber are as follows:

- Un-sprung weight is reduced as the pressurized gas takes up part of the vehicle weight.
- It can be fitted in any orientation *i.e.*, upside down arrangement is possible.
- It runs cooler because the heat is dissipated directly to the atmosphere through the single tube.
- Tube is much longer which restricts its use in the passenger cars.
- As there is only one tube inside which piston is reciprocating, any damage to this tube will damage the entire unit.
- The pressure used is very high (360 psi).
- Poor performance as compared to the twin-tube shock absorber.

1.5 CONTRIBUTION OF THE THESIS

The contribution of the thesis is as follows:

- Experiment is done on the slotting machine to give external excitation to the shock absorber and temperature development at the surface is measured with the use of thermo-couples.
- The bond graph model for the pressure development in the two chambers of the shock absorber is developed.
- The developed pressure is given as input to obtain the bond graph model for volume flow rate of hydraulic fluid through the piston valve of the shock absorber.
- The detailed bond graph model for the temperature development of the shock absorber fluid is developed and it is shown that temperature development is a function of volume flow rate of fluid through the piston valve.
- Material properties of the shock absorber are included in the bond graph model for temperature development to calculate the surface temperature of shock absorber.
- Saturation point is found for different stroke lengths of piston which marks the point of maximum dissipation of heat to the surroundings.
- Comparison between the temperature at the surface of shock absorber for the experiment and simulation is done.

1.6 ORGANIZATION OF THE THESIS

Five chapters are included in this Thesis. Overview of the various chapters is as follows:

First chapter includes the introduction part, role of shock absorber in the suspension system of the vehicle, various types of shock absorbers and comparison is made between the mono-tube and twin-tube shock absorber.

Literature review related to different modeling techniques for hydraulic shock absorber is included in the second chapter. Various developments in the shock absorbers to enhance the comfort level and control over the vehicle are given in the literature. Literature gap and objective of this thesis are also included in this chapter.

Basic principles of Bond Graph and its applications in modeling of thermal systems are given the third chapter. This chapter also includes the basic bond graph model and thermal bond

graph model for twin-tube shock absorber. Simulation results for pressure development, temperature development and volume flow rate of hydraulic fluid are presented.

Fourth chapter includes the experimental setup. Experimental setup consists of slotting machine, twin-tube shock absorber, thermo-couples for temperature measurement and dynamometer for the input force measurement. Comparison between the simulation results and experimental results is also included in this chapter.

Conclusion and scope for future work is presented in the concluding chapter.

2.1 INTRODUCTION

The literature review on Bond Graph modeling, shock absorber modeling, literature gap and objective of the thesis are presented in this chapter. The Bond Graph is a modeling and simulation technique that can satisfactorily simulate the complex systems consisting of sub-systems with different energy domains. Literature regarding different elements of Bond Graph and their applications to construct the Bond Graph for any system are discussed. Next, the research conducted to determine the various performance characteristics of twin-tube shock absorber is presented. Various researchers have developed different model for predicting the performance of twin-tube shock absorber. Various strategies are suggested to enhance the ride comfort, vehicle stability and to have better control over the steering and braking system of the vehicle.

2.2 APPLICATIONS OF BOND GRAPH MODELING

System dynamics that can be represented by graphical modeling technique is called Bond Graph. Systems with different energy domains can be identified with the use of Bond Graph. Bond Graph is a more dominant technique for modeling systems consisting of sub-systems with different energy domains. Any physical system can be represented by predefined elements of Bond Graph [3–5].

Mechatronic systems can be designed by using the Bond Graph and fault estimation, identification and diagnosis can also be done. Modeling and simulation play a very important role in engineering science. Any physical system can be represented in terms of system of equations describing the behavior of the system. Some systems become very complex and it becomes impossible for such systems to derive differential equations. For such systems, Bond Graph plays an important role. In Bond Graph, there is need to draw bonds connecting the different elements of the system and the differential equations describing the system are obtained automatically by software. In this way, complex system simulation can be done more easily with Bond Graph [6–9].

The pseudo Bond Graph model for a thermo-hydraulic system composed of two pipes (cold water and warm water pipe), evacuation pipe and a plastic tank was described in [10].

Efficiency of Bond Graph model was shown by simulating the model for variable and constant mass flow rates of water. Model satisfactorily showed the power transfer and coupling of hydraulic system with the thermal system. Dynamic equations and constitutive relations were developed from the Bond Graph model which was drawn in accordance with the direction of energy flow. Dependence of temperature variation on the mass flow rate of cold and warm water was shown by the simulation results. Efficiency of the Bond Graph model was tested using constant and variable mass flow rates.

The difference between conventional Bond Graphs and convective Bond Graphs for thermal systems is very important [11]. It was found difficult to simulate the thermodynamic systems with the use of conventional Bond Graphs. A convection bond was described to simulate the thermodynamic systems which were difficult to simulate by conventional Bond Graphs. Two effort variables were used which were independent of each other as opposed to the use of single effort variable for each bond in case of conventional Bond Graphs. The use of two independent efforts was denoted by dashed line drawn parallel to a solid line.

In Bond Graph, the only requirement is to convey some essential information of the system to the computer [12]. This information needs to be conveyed in an unambiguous manner so that, every information that is conveyed to the computer can follow some algorithmic procedure to derive the required differential equations. So, the main idea in Bond Graph is to formulate some kind of language in which the essential characteristics of the system can be conveyed to the computer so that it can follow an algorithmic procedure which is already programmed into it in order to derive the differential equations.

2.3 SHOCK ABSORBER MODELING

A mathematical model to foretell the thermal characteristics of hydraulic twin-tube shock absorbers was developed in [13]. The shock absorber was divided into 17 subsystems *i.e.*, rebound chamber, reserve chamber *etc.* Each subsystem was taken as control volume and energy conservation equation was applied to each subsystem. So, 17 first order non-linear differential equations were obtained. Euler's method was used to integrate these differential equations. Position and speed were taken as the inputs to the system. Thermal stability conditions were taken for simulating the model. Experiment had been conducted on the 4 shock absorbers and the temperature at stabilization was measured. Stabilization temperatures between the model and

experiment were compared. The relative percentage error for the reserve chamber stabilization temperature was less than 15% for all the shock absorbers. The highest difference between the experimental and model results was approximately 20%. Heat transfer from shock absorber to the test machine by conduction was not considered.

Physical and mathematical model for twin-tube hydraulic shock absorber, using oil as the hydraulic fluid play a vital role in predicting the properties of hydraulic shock absorber [14]. Equations for the alteration of oil pressure in different chambers were derived. Fourth and fifth order Runge-Kutta method based algorithm was used to solve the various differential equations. Graphs between the damping force and relative displacement of piston for different values of amplitude and frequency of excitation were obtained. It was analyzed that the damping force characteristics depends mainly on the geometrical configuration of the bottom and top piston valves of the shock absorber. Maximum ride comfort characteristics were obtained and it was suggested that the mass flow rate of hydraulic fluid should be low during the rebound stroke as compared to the compression stroke.

A displacement sensitive orifice in the twin-tube shock absorber is a new advancement in shock absorbers evolution [15]. Displacement sensitive shock absorber was proposed to increase the ride comfort and to enhance the control over the vehicle. The soft, hard and transient zones were determined for the displacement sensitive shock absorber. Continuity equations for flow were derived for the compression and the rebound chamber. Equations for mass flow rates during the compression stroke and rebound stroke were also obtained. Damping action given by the shock absorber was determined by considering the various forces acting on two sides of the piston. Taking the damping force on the Y-axis and piston displacement on the X-axis, graphs were obtained by simulating the various equations. Similar trend between the experiment and the simulation results were observed. It was suggested that the enhanced ride comfort can be achieved using DSSA (Displacement sensitive shock absorber) as compared to simple twin-tube shock absorber.

Shock absorber works on the principle of converting the kinetic energy into heat energy when there is flow of oil through the piston valve and base valve [16]. The piston valve and base valve resists the flow of oil through them and thus provides the damping action. While doing so, the hydraulic fluid gets heated. This heat has a tendency of altering the properties of the shock absorber fluid which could adversely affect the performance of shock absorber. Heat dissipates

to the outside atmosphere through gas contained in the reserve chamber. This gas was replaced with various other fluids such as turpentine, methanol and water that have a higher thermal conductivity than air. Heat transfer rates considering only conduction were calculated for turpentine, methanol and water. Temperatures at the different sections of the shock absorber were measured experimentally with the use of thermo-couples. Experiment was conducted at the shock absorber test rig. Temperature was measured for air, water, methanol and turpentine. Maximum heat transfer was recorded for methanol as the thermal conductivity of methanol is highest among the used fluids.

The mathematical model for the twin-tube shock absorber was developed and simulation was done with the Easy5 software [17]. The model was established according to the internal configuration of twin-tube shock absorber. Small deflection theory was used to study the ring throttle. The bench test for the shock absorber was done. Correlation data for the damping force indicates that the percentage relative error between the experiment and the simulation data was less than 10%. Velocity characteristics diagram and indicator diagram showed the similar trend for the experiment and simulation. It was suggested to study the model further to know the dynamic characteristics of the shock absorber and their impact on the dynamic performance of the vehicle.

Another technique to develop a mathematical model is with the help of data collected from experiments and then using a Back-Propagation (BP) neural network technique [18]. Inputs to the BP neural model are the characteristic parameters of the shock absorber and the output was damping force. High accuracy was attained with this model as it is experimental based model. All the factors affecting the performance of shock absorber in real situation were considered while doing the experiment.

A very effective method to predict the performance of shock absorber is a use of triangular displacement signals as input excitation to the piston of the shock absorber having constant velocity of excitation [19]. Steady state characteristics of shock absorber were identified by robust automated technique. Force-velocity curves were obtained that serves as an effective tool in various tasks of damper analysis such as validation of model, performance monitoring of shock absorber, refinement of model. Deep examination for the feasibility of this technique was done when the transient pressure variations were present. Excitation velocities step changes are the main reason behind the creation of the transient pressure variations and there occurs a

problem in identifying the steady state characteristics of the shock absorber. It is shown that the step changes in the external excitation velocity occurred due to compressibility of hydraulic fluid, flexibilities in material of shock absorber. It was shown that the responses from the shock absorber model were unsteady to a very little amount throughout the complete stroke of the piston. The conditions for which the response nears steady state had been examined for turbulent, laminar and mixed flows. It is found that the steady flow conditions worked remarkably well for various test configurations, which made it possible to this technique for identifying the steady state characteristics of the shock absorber. A lag damper, which is a device utilized in helicopters for the purposes of stability, was tested with this methodology.

Damper analysis and suspension analysis play an important role in vehicle stability. These two analyses were used to attain the efficient monitoring of the condition of shock absorbers under normal operation of vehicle [20]. Pressure, temperature and acceleration sensing were used to determine the condition of shock absorber and hence, there is a scope for future accomplishment of projects based on low cost fabrication. It was shown that the efficient monitoring device can be fitted on the damper body which can determine the status of shock absorber continuously while the vehicle is in operation and hence real time diagnosis can be carried out. It was concluded that the development of such monitoring device could reduce the risk of vehicles running with the defective shock absorbers and thus, the overall safety of the rider and vehicle can be achieved.

The amplitude-selective-damping (ASD) valve in the simple twin-tube shock absorber was described. Affects of the ASD valve on the performance characteristics of twin-tube shock absorber were obtained. Mathematical model for the ASD valve was also developed [21]. Damper base characteristics were obtained and various applications of ASD were discussed.

A mathematical model to determine the damping force and dependence of damping force on the geometry of orifice and number of shims used was developed. It was considered that the damping force is linear in nature [22]. Damping force of the twin-tube shock absorber depends on the geometrical properties of the piston orifice and physical properties of the hydraulic fluid. Stiffness of shims, which were used to control the flow rate through the piston orifice, was determined by finite element analysis. Pressure difference between the upper chamber and lower chamber of twin-tube shock absorber was calculated using the Matlab program simulating the

model based on the continuity equations of fluid flow. It was found that the damping force reduces with the increase in the mass flow rate of hydraulic fluid through the shock absorber.

A mathematical model based on experiment was extended for predicting the various properties of the twin-tube shock absorber [23]. The input parameters to this model were taken from the experimental data. Experiment was conducted for three different frequencies with an excitation of 1, 3 and 12 Hertz. Then the experimental results and simulation results were compared to validate the model. Finally the output characteristics were obtained for the shock absorber included in the quarter car model and results were compared to the real road conditions.

A model to determine the damping force of the twin-tube shock absorber considering the affect of heating of hydraulic fluid was presented [24]. Results for the damping force were obtained by simulating the model considering the thermal effects. It was found that the damping force varies considerably due to heating of hydraulic fluid and it adversely affects the performance of the shock absorber. Variation of temperature with time was also measured. Results for the damping force obtained by this model were compared with the results of damping force without considering the thermal effects.

The method to determine the mechanical behavior of shock absorber under dynamic load conditions which were time dependent was discussed in [25]. In this method, the vehicle was considered as mechanism consisting of rigid bodies which were connected by bushing, springs, joints and dampers. Non-linearity of damping force was considered. Heat generation during the working of shock absorber adversely affect the properties of the hydraulic fluid. These affects became much more dangerous while riding on the long rugged road. Hence, thermo-mechanical model was developed describing the performance of shock absorber with a fairly good approximation for the conditions of rough road. Thermo-mechanical performance of two shock absorbers was discussed in detail to validate the above theory. Dependence of the force on the velocity was measured for different temperatures of the hydraulic fluid. Temperature of rear and front shock absorber was recorded for the real road conditions. Experimental results were compared with simulation results and greater convergence of results was achieved.

A black box model for identification of a continuously varying, electro-hydraulic shock absorber of a passenger car was advancement in the field of shock absorber simulation [26]. Structure of neural network output error model was utilized to describe the non linearity of the damper. Regression vector, model parameters and optimum experiment design are estimated for

identification of the system. Simulation was done using both *i.e.*, the optimized excitation as input and the random phase sine wave as input excitation and it was found that better results were obtained in case of optimized excitation as input.

The experimental study and the control system for the semi-active rear shock absorber of a motor cycle were developed in [27]. Electro-hydraulic control was used to properly monitor the shock absorber. This electronic control system was used on the motorcycle and performance characteristics were noted for the real road conditions. Test bench results were compared with the results obtained in the real road conditions and a better convergence of results were obtained.

The method to predict the optimum performance of a shock absorber in the suspension system with main emphasis on the vehicle handling control was developed in [28]. Quarter car model was used with a damper which can be monitored and mixed integer programming theory was used. Better performance regarding comfort was achieved for the shocks of low frequency and comfort level was reduced with the increase of frequency. It was suggested to have optimum monitoring of the damper in order to enhance the comfort level at increased frequency.

The magneto-rheological dampers were used in the suspension system with adaptive semi active control [29]. Two adaptive control methods were discussed in the proposed model *i.e.*, adaptive reference control and adaptive inverse control. Adaptive inverse method was used to control the hysteretic non linear dynamics for the magneto-rheological damper which can be apprehended by identifying the forward model of the magneto-rheological damper. Reference damping force was generated with the use of input voltage. Required damping force was applied to the reference dynamics through adaptive reference control.

The control system for the semi-active suspension system and vehicle dynamic control system was developed based on the integrated control theory [30]. Shock absorber monitoring was done to have a greater control over the suspension system and to enhance the ride performance of the vehicle. Vehicle dynamics control (VDC) was employed to increase the stability of the vehicle by providing the traction control. Dynamics performance of the vehicle was predicted by simulating the vehicle dynamics model which was based on ADAMS. Matlab Simulink was employed to establish the skyhook controller.

The basics characteristics of active, semi active and passive vehicle suspension system can be categorized [31]. Basic characteristics were investigated by giving real road surface conditions as input external excitation to the vehicle model. Passive and active suspension

systems were modeled by using linear analysis method and semi-active suspension system was modeled with the help of non-linear analysis. Optimal parameters of the active suspension system were determined by using theory of linear optimal control. Optimum active parameters were used to evaluate the performance of the semi active suspensions.

2.4 LITERATURE GAP

After doing detailed study of literatures of different models of vehicle shock absorber, it is known that many researchers have worked on twin-tube hydraulic shock absorbers. Models were developed to predict the performance characteristics. From the literature review, it is clear that the performance of shock absorber depends to a great extent on the ability of shock absorber to dissipate heat to the surroundings so that the fluid used does not get heated up to an extent that may affect the performance of shock absorber. But, very less work is carried out to predict the thermal behavior of shock absorber. So, there is a need to work on the Thermal modeling of twin-tube hydraulic shock absorber.

2.5 OBJECTIVE OF THE PRESENT WORK

From the literature review, it can be established that Bond Graph plays a very important role in modeling and simulating the complex systems. Thermal model of twin-tube shock absorber can be developed with the use of Bond Graph technique. Thermal Bond Graph model for such a system has not developed yet. So, the objective of this thesis is summarized below:

- To study the working of twin-tube shock absorber experimentally and to measure the input force and temperature variation with time.
- To develop the Bond Graph model for the pressure development in the two chambers of the shock absorber.
- To develop the Bond Graph model measuring the volume flow rate of hydraulic fluid through the piston orifice and its impact on the damping force and temperature development in upper chamber and lower chamber.
- To develop the detailed Bond Graph model for the temperature development of the shock absorber fluid.
- To validate the thermal Bond Graph model by comparing the experimental data with the results obtained by simulation.

3.1 INTRODUCTION

Generally, there is need to obtain differential equations for solving different engineering problems encountered in a day to day life. Linear differential equations can be solved analytically. But in most of the engineering problems the equations to be solved are non-linear differential equations. For solving these equations, it is very difficult to have an analytical solution. So, there is need to obtain a numerical solution for such equations. In all the available techniques, the differential equations are written by human and then it is the job of the computer to solve the equations. The differential equations can be automatically generated by modelling the system with the help of Bond Graph modelling technique. In this chapter, Bond Graph is used to develop the thermal model of hydraulic shock absorber with different stroke lengths. Temperature variation, pressure rise and volume flow rate of oil in the upper chamber and lower chamber of shock absorber are modelled. Two thermal C-fields may be used to predict the temperature of oil in the upper chamber and lower chamber.

3.2 BOND GRAPH

In Bond Graph the only requirement is to convey some essential information of the system to the computer. This information needs to be conveyed in an unambiguous manner so that, every information that is conveyed to the computer can follow some algorithmic procedure to generate the required differential equations. So, the main idea in Bond Graph is to formulate some kind of language in which the essential characteristics of the system can be conveyed to the computer so that it can follow an algorithmic procedure which is already programmed into it in order to derive the differential equation. Now, the question arises that what are the essential characteristics that are to be conveyed to the computer.

In any system, there are elements such as capacitive, resistive and inertial elements that make up the whole system. Now, it is important to know the nature of interaction between these elements. They interact essentially by exchanging energy. For example, if there is a resistor in the circuit, it absorbs energy and then dissipates it into the environment. In a nutshell, it is the

energy that is exchanged between different elements of the system residing in different energy domains. Further, it is not only the energy but also the information that is exchanged between the elements of the system. Basically, energy per unit time is a power and this power is composed of two variables *i.e.*, effort and flow. It is a product of effort variable and flow variable. In case of mechanical system, the effort variables are force, torque and the flow variables are linear and angular velocity. Likewise, the effort variable and flow variables for different systems are shown in Table 3.1.

Table 3.1: Power Variables in Different Energy Domains [8]

Systems	Efforts (e)	Flow (f)
Mechanical	Force (N)	Velocity ($\text{m}\cdot\text{s}^{-1}$)
	Torque (N·m)	Angular velocity ($\text{rad}\cdot\text{s}^{-1}$)
Hydraulic	Pressure ($\text{N}\cdot\text{m}^{-2}$)	Volume flow rate ($\text{m}^3\cdot\text{s}^{-1}$)
Electrical	Voltage (V)	Current (A)
Thermal	Temperature (K)	Entropy change rate ($\text{W}\cdot\text{K}^{-1}$)
	Pressure ($\text{N}\cdot\text{m}^{-2}$)	Volume change rate ($\text{m}^3\cdot\text{s}^{-1}$)
Chemical	Chemical potential ($\text{N}\cdot\text{m}\cdot\text{mol}^{-1}$)	Mass flow rate ($\text{mol}\cdot\text{s}^{-1}$)
	Entropy (Q/K)	Mass flow rate (kg/s)
Magnetic	Magnetic-motive force (An)	Magnetic flux rate ($\text{Wb}\cdot\text{s}^{-1}$)

So, in every domain, wherever the dynamics take place, there is effort and flow variable. As already discussed, there is a power exchange between different elements of the system and this power is the product of flow and effort variable. But the information about the effort and

flow variable should also be exchanged between different elements of the system, these are called information variables. So, flow and effort are called information variables and their product is a power variable. It is the exchange of these information and power variables between the elements of the system which explains the dynamics of the system. This exchange of information variables and power variables can be represented in the form of graphic representation. This graphic presentation conveys the essential characteristics of the system to the computer which further derives the differential equations based on the algorithm. So, Bond Graph is nothing but a pictorial representation of exchange of information and power variables.

3.2.1 Elements of Bond Graph

There are various elements used in the Bond Graph that can make up the whole system in every energy domain. The basic elements in the Bond Graph theory are as follows:

- **Basic 1- port elements:**

1. The inertial element (I): This element gives the relationship between the effort and flow in such a way that integration of effort gives the flow. For example, mass in mechanical system and inductor in electrical system acts as inertial elements. The basic characteristic of inertial element is as follows:

For electrical system:

$$V = L \frac{di}{dt} \quad (3.1)$$

$$i(t) = \frac{1}{L} \int_{-\infty}^t V dt \quad (3.2)$$

For mechanical system: Force = rate of change of momentum

$$e = \frac{dP}{dt} \quad (3.3)$$

$$P(t) = \int_{-\infty}^t e dt \quad (3.4)$$

So, it can be written in general form:

$$\text{Flow} = (\text{a constant or a function}) \times \int_{-\infty}^t (\text{effort}) dt \quad (3.5)$$

2. The compliant element (C): The constitutive relation for this element is just opposite to that of the inertial element. Here, the relation between the flow and effort is such that the integration of flow gives the effort. For example, capacitor in electrical system and the spring in mechanical system act as compliant element.

For electrical system:

$$i = C \frac{dV}{dt} \quad (3.6)$$

$$V = \frac{1}{C} \int_{-\infty}^t i dt \quad (3.7)$$

In general terms: Effort = (a constant or a function) $\times \int_{-\infty}^t$ (flow) dt

3. Resistive element (R): This element is very much different from I or C elements and involves no integration. It gives a direct relationship between flow and effort variable. For example, resistor in electrical system and damper in mechanical system act as a resistive element. Mathematically, the characteristic equation for resistive element can be written as follows:

$$\text{Effort} = (\text{a constant or a function}) \times (\text{Flow}),$$

$$\text{Flow} = (\text{a constant or a function}) \times (\text{Effort}).$$

4. Source of effort (Se): It is the external effort applied on the system and the system does not have any effect on its output. The property of this element is that it can independently decide the effort variable on a bond associated with it, but it cannot decide a flow variable, the flow variable being decided by the rest of the system. For example, source of effort in electrical system is voltage and it is force in case of mechanical system.

5. Source of flow (Sf): It can independently determine the flow variable, the effort variable being decided by the rest of the system. For example, current in electrical system and motion of cam in mechanical system is a source of flow.

Basic 2-port elements:

1. Transformer: It neither stores nor dissipates energy. Like in the electrical circuit, transformer do the job of stepping up or stepping down the voltage, it is same in Bond Graph, transformer can transduce efforts to efforts and flows to flows. Let the flow f_j is n times flow f_i . Here n is known as the modulus of the transformer. A transformer is represented as shown in Fig. 3.1.

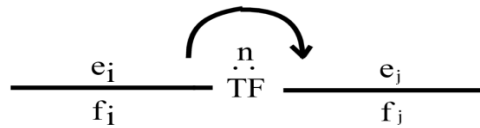


Fig. 3.1 Bond Graph for Transformer

It gives: $f_j = n f_i$ and $e_i = n e_j$

The way in which a modulus is defined, is indicated by the orientation of the arc. The modulus is declared according to the transformation of flow to flow. The transformation relation for effort to effort is in the direction opposite to that of flow to flow transformation.

2. Gyrator: Like transformer, it is also a 2-port element in Bond Graph. It gives a relation between effort to flow and vice-versa, but the power remains same on the port. Hence, the power remains conserved. For example, mechanical gyroscope acts as a gyrator. In gyroscope, force in vertical direction generates a motion in direction perpendicular to this force *i.e.*, in a horizontal direction and a force in a horizontal direction is required in order to maintain a motion in vertical direction. Thus, there is a transformation of flow into effort and vice-versa. A gyrator in Bond Graph is represented as shown in Fig. 3.2.

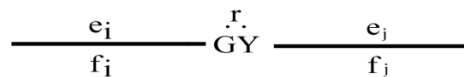


Fig. 3.2 Bond Graph for Gyrator

Here, r is known as gyrator modulus. The definition of modulus is from flow to effort.

In general form, flow and effort in gyrator are related as follows:

$$e_j = r f_i \text{ and } e_i = r f_j$$

Apart from these seven elements, there are two more elements. These two elements are 3-port elements. These are called junction 1 and junction 0.

3.2.2 Junctions

There are two types of junctions used in Bond Graph *i.e.* 0-junction and 1-junction.

1. 0-junction: Algebraic sum of flows are zero in this junction and there is common effort on the bonds attached to this 0-junction. This junction is also called flow sum junction. The half arrow attached to each bond gives the sign to be used while taking algebraic sum. This corresponds to a node in an electrical circuit or to a mechanical "stack" in which all the forces are equal. In 0-junction, the flow and the efforts satisfy the expressions (3.8) and (3.9) as given below:

$$\sum \text{Flow}_{\text{input}_n} = \sum \text{Flow}_{\text{output}_m} \quad (3.8)$$

$$\text{Effort}_{\text{input}_1} = \text{Effort}_{\text{input}_2} = \dots = \text{Effort}_{\text{input}_n} = \text{Effort}_{\text{output}_1} = \text{Effort}_{\text{output}_2} = \dots = \text{Effort}_{\text{output}_m} \quad (3.9)$$

This corresponds to a node in an electrical circuit (where Kirchhoff's current law applies).

2. 1-junction: The algebraic sum of efforts at the junction is zero, hence it is also known as effort sum junction. There is common flow in the Bonds attached to this junction. This corresponds to an electrical loop or to a force balance at a mass in a mechanical system. In a 1-junction, the flow and the efforts satisfy the expressions (3.10) and (3.11) as given below:

$$\sum \text{Effort}_{\text{input}_n} = \sum \text{Effort}_{\text{output}_m} \quad (3.10)$$

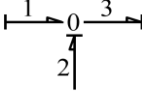
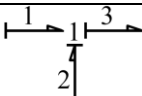
$$\text{Flow}_{\text{input}_1} = \text{Flow}_{\text{input}_2} = \dots = \text{Flow}_{\text{input}_n} = \text{Flow}_{\text{output}_1} = \text{Flow}_{\text{output}_2} = \dots = \text{Flow}_{\text{output}_m} \quad (3.11)$$

This corresponds to force balance at a mass in a mechanical system. An example of a "1" junction is resistors in series. In junction, the premise of energy conservation is assumed, no lost is allowed.

Once the system is represented in the form of Bond-Graph, the required essential information will be conveyed to computer through this Bond-Graph and the differential equations describing the system under consideration will be generated directly in terms of generalized variables defined above, using simple and standardized procedures, regardless of the physical domain to which it belongs. Bond Graph uses a set of elements to model the real system as shown in Table 3.2.

Table 3.2: Bond Graph elements [8]

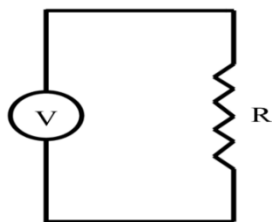
Type	Name	Symbol	Definition	
			Linear	Nonlinear
Storages	Inertia		$f = \frac{1}{m} \int_{-\infty}^t e \, dt$	$f = \psi_I \left(\int_{-\infty}^t e \, dt \right)$
			$e = m \frac{df}{dt}$	$e = \phi_I \left(\frac{df}{dt} \right)$
	Capacitance		$e = K \int_{-\infty}^t f \, dt$	$e = \phi_C \left(\int_{-\infty}^t f \, dt \right)$
			$f = \frac{1}{K} \frac{de}{dt}$	$f = \psi_C \left(\frac{de}{dt} \right)$
Dissipation	Resistance		$f = e/R$	$f = \psi_R(e)$
			$e = Rf$	$e = \phi_R(f)$
Transducers (ideal)	Gyrator I		$e_2 = r f_1$ $e_1 = r f_2$	$e_2 = r(x) f_1$ $e_1 = r(x) f_2$
	Gyrator II		$f_1 = \frac{1}{r} e_2$ $f_2 = \frac{1}{r} e_1$	$f_1 = \frac{1}{r(x)} e_2$ $f_2 = \frac{1}{r(x)} e_1$
	Transformer I		$f_2 = \mu f_1$ $e_1 = \mu e_2$	$f_2 = \mu(x) f_1$ $e_1 = \mu(x) e_2$
	Transformer II		$f_1 = \frac{1}{\mu} f_2$	$f_1 = \frac{1}{\mu(x)} f_2$

			$e_2 = \frac{1}{\mu} e_1$	$e_2 = \frac{1}{\mu(x)} e_1$
Sources	Source of effort	SE \longrightarrow	$e = e(t)$	
	Source of flow	SF \longleftarrow	$f = f(t)$	
Junctions	Zero (0)		$e_1 = e_2 = e_3$ $f_1 + f_2 = f_3$	
	One (1)		$f_1 = f_2 = f_3$ $e_1 + e_2 = e_3$	

3.2.3 Causality

The different elements of Bond Graph and their usage is already discussed. Now, having known that no single element can decide both flow and information variables, while drawing a Bond Graph, the information to be conveyed to computer should follow in a very specific direction. How this information is flowing and in which direction it is flowing, are controlled by a causality.

To illustrate, let the voltage source connected to a resistor in series as shown in Fig. 3.3 (a). So, the Bond Graph for this network is source of effort (Se) and resistance (R) connected to 1-junction.



(a)



(b)

Fig. 3.3 (a) Electrical circuit having voltage source and resistor and (b) causalled Bond Graph for the circuit

Now, the voltage source decides the effort but it cannot decide the flow information. Resistance (R) in this particular case, decides the flow information. So, effort is going from the voltage source (Se) towards resistance (R) and resistance (R) is sending back a flow information towards voltage source (Se). This is shown in Fig. 3.4(b). Here the half arrows are used to show the power direction. Elaborate discussion on the causality of all elements of Bond Graph is given below.

1. Causality of source of effort (Se): It gives the information of effort to the rest of the system and receives the flow information from the rest of the system. A stroke is put at an end of the Bond which is receiving the effort information. It can be represented as shown in Fig. 3.4.



Fig. 3.4 Causality of source of effort

2. Causality of source of flow (Sf): It provides the information of flow to the rest of the system and receives the effort information from the rest of the system. The end of the Bond at which flow is received is an open. Causality of Sf element is shown in Fig. 3.5.



Fig. 3.5 Causality of source of flow

3. Causality of inertial element (I): In order to understand the causality of inertial element, it is important to have the knowledge of characteristic of inertial element.

$$\text{Flow} = (\text{a constant or a function}) \times \int_{-\infty}^t (\text{effort}) dt$$

It means, inertial element needs to have the information about the effort in order to generate the flow information. So, for this element, effort is the cause and flow is effect. Inertial element can be represented as shown in Fig. 3.6.



Fig. 3.6 Integral Causality of inertial element

4. Causality of compliant element (C): Causality of this element is just the opposite of causality of inertial element. To understand this, it is important to know about the basic characteristic of compliant element.

$$\text{Effort} = (\text{a constant or a function}) \times \int_{-\infty}^t (\text{flow}) dt$$

So, in this case, the history of flow information should be known in order to have a effort information. In this way, flow is a cause and effort is an effect for the compliant element. Causality of compliant element is shown in Fig. 3.7.



Fig. 3.7 Integral Causality of compliant element

The causality discussed for I and C element is called integral or proper causality. Sometimes the stroke is inverted in these elements. Such a causality is called differential causality or improper causality.

5. Causality of resistive element (R): There occurs no integration in case of this element. This element gives a direct relation between flow and effort. So, in this element, flow can act as cause as well as effect. At the same time, effort can also act as cause as well as flow. When the flow acts as cause, the effort will act as an effect and vice-versa.

To understand this, consider a voltage source connected to the resistor as shown in Fig. 3.8(a). In this case, the effort will act as cause and flow as effect for R element as shown in Fig. 3.8(b).

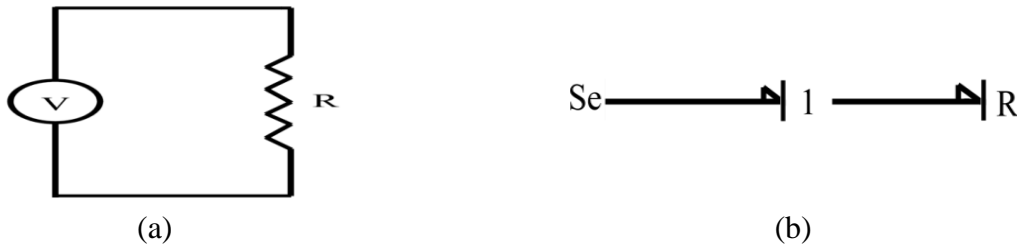


Fig. 3.8(a) Electrical circuit having source of effort and (b) causality of resistive element when it receives effort

Now, consider current source connected to resistor R as shown in Fig. 3.9(a). In this case, the effort will act as effect and the flow as cause for R element as shown in Fig. 3.9(b).

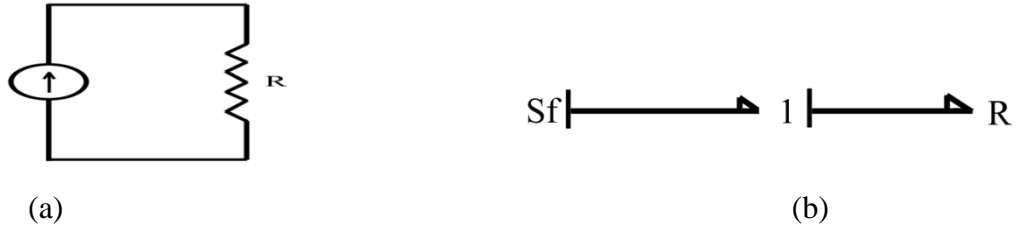


Fig. 3.9 (a) Electrical circuit having source of flow and (b) causality of resistive element when it receives flow

6. Causality of transformer element (TF): There are possibilities for the causation of this element. If the flow information is from left to right, then the causality of TF element will be as shown in Fig. 3.10.

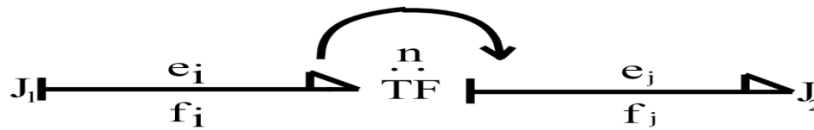


Fig. 3.10 Causality of transformer element when flow is from left to right

If the flow information is from right to left, then the causality of TF element will be as shown in Fig 3.11.

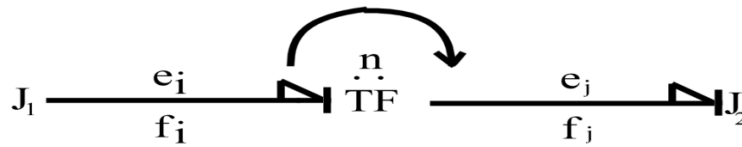


Fig. 3.11 Causality of transformer element when flow is from right to left

7. Causality of gyrator element (GY): Characteristic of GY element is that the effort in one bond of gyrator is proportional to flow in other bond and vice-versa. So, the causality of this element can be represented in two ways as shown in Fig. 3.12.

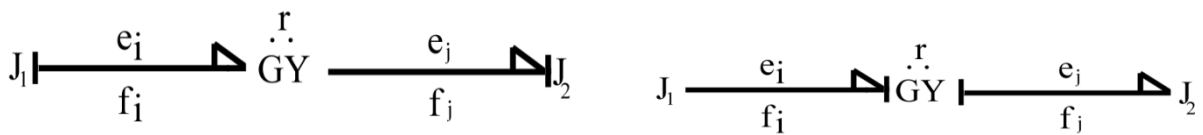


Fig. 3.12 Causality of gyrator element

8. Causality of junction elements: 0-junction is a flow sum junction or a common effort junction. So, only one bond has an effort stroke at the end which is towards the 0-junction while the other bonds will be flow-caused in the direction towards the junction. The only bond which has an effort stroke at the end which is towards the 0-junction, is known as a strong bond. Causality of 0-junction is shown in Fig. 3.13.

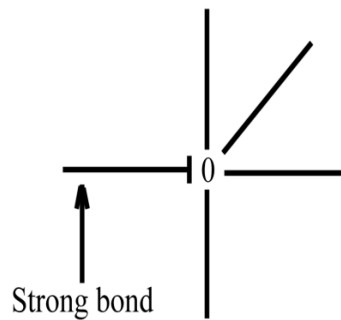


Fig. 3.13 Causality of 0-junction

Similarly, in case of 1-junction, the flow is common to all bonds, but the sum of efforts at the junction is zero. So, except one bond, all other bonds have an effort stroke towards the 1-junction. The only bond which has an effort stroke away from the 1-junction, is known as a strong bond for 1-junction. Causality of 1-junction is shown in Fig. 3.14.

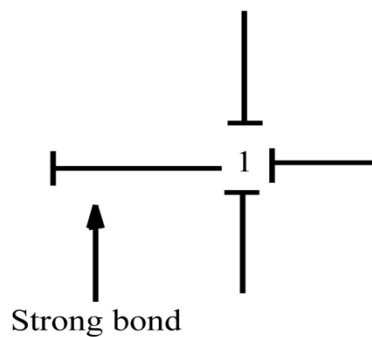


Fig. 3.14 Causality of 1-junction

9. Differential causality: The proper or integral causal orientation of C and I elements is already discussed. But sometimes, the position of stroke is inverted or it is said that the effort and flow information follow the differential equation instead of an integral equation. So, for I element, the flow becomes cause and the effort becomes effect. This is just opposite of integral causality and

is known as differential causality or improper causality. Differential causality for I element is shown in Fig. 3.15.



Fig. 3.15 Differential causality of I element

Similarly, in case of C element, effort becomes the cause and flow becomes the effect in case of differential causality. So, the differential causality for C element can be represented as shown in Fig. 3.16.



Fig. 3.16 Differential causality of C element

3.2.4 Bond Graph applied to Thermal System

Consider a chamber whose walls are thermally conducting. There is a hole at the bottom of this chamber which allows the gas to leave out or enter into the chamber. So, there is control volume having gas inside it.

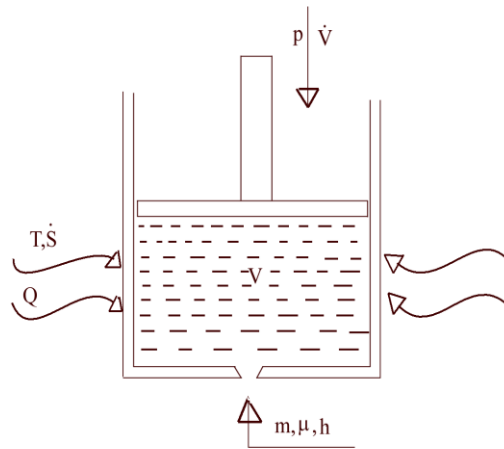


Fig. 3.17 Control volume with thermally conducting wall containing gas

The internal energy in this control volume (V) can be expressed in terms of chamber volume, total entropy and gas mass inside the chamber. Gas is assumed as ideal.

$$U = U(V, S, m) \quad (3.12)$$

Here U = internal energy, V = chamber volume, S = total entropy, m = total mass of the gas inside the chamber. The time rate of change of internal energy can be written as

$$\dot{U} = \frac{\partial U}{\partial V} \dot{V} + \frac{\partial U}{\partial S} \dot{S} + \frac{\partial U}{\partial m} \dot{m} \quad (3.13)$$

Now from First law of Thermodynamics, it can be written as

$$\frac{\partial U}{\partial V} = -p, \quad \frac{\partial U}{\partial S} = T, \quad \frac{\partial U}{\partial m} = \mu$$

where p is thermodynamic pressure, T is absolute temperature and μ is chemical potential. A proposed C- field is shown below in Fig. 3.18.

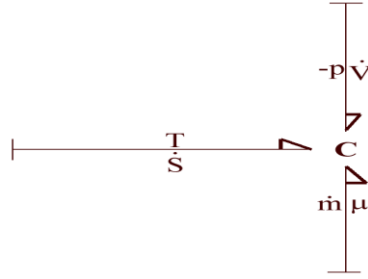


Fig. 3.18 A basic thermal C-field

There are three ports in this C-field. Here, the rate of change of volume (V) acts as a flow variable and the pressure (p) acts as effort variable for the hydraulic port. Similarly, the rate of change of entropy (S) acts as flow variable and temperature (T) of the gas effort variable acts as effort variable for thermal port. The mass flow rate acts as flow variable and chemical potential (μ) acts as effort variable for material port. Now, since entropy(S) is an extensive quantity, thus it can be written as $S = ms$, where s is the entropy per unit mass. Hence,

$$\dot{S} = \dot{m}s + m\dot{s} \quad (3.14)$$

In the above equation, there are two components of entropy change. The first component denotes the entropy change because of mass transfer and second component denotes the entropy change because of the fact that heat is transferred to the control volume containing gas. Thus

$$\dot{S} = \dot{m}s + \dot{S}_{ht} \quad (3.15)$$

Now, the Bond Graph drawn earlier may be modified to represent the above equation for the entropy change as shown in Fig. 3.19

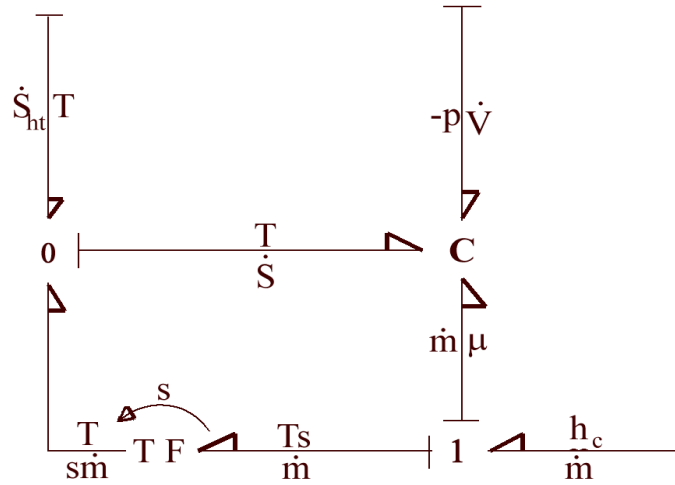


Fig. 3.19 Modified Thermal C-field

Now, considering h_c as the effort for the material port, then

$$h_c = \mu + Ts \quad (3.16)$$

For the system where the composition is not constant, internal energy will be a function of entropy change, volume change and composition change. So, change in internal energy can be written as

$$U = U(S, V, m) \quad (3.17)$$

$$dU = \left(\frac{\partial U}{\partial S} \right)_{V, m} dS + \left(\frac{\partial U}{\partial V} \right)_{S, m} dV + \left(\frac{\partial U}{\partial m} \right)_{S, V} dm \quad (3.18)$$

$$dU = TdS - pdV + \left(\frac{\partial U}{\partial m} \right)_{V, S} dm$$

$$dG = Vdp - Sdt + \left(\frac{\partial G}{\partial m} \right) dm \quad (3.19)$$

Now, Gibbs free energy can be written as function of pressure, temperature and composition. Since $G=U+pV-TS$

$$d(U + pV - TS) = Vdp - SdT + \left(\frac{\partial G}{\partial m}\right)dm \quad (3.20)$$

$$\Rightarrow dU + pdV + Vdp - TdS - SdT = Vdp - SdT + \left(\frac{\partial G}{\partial m}\right)dm$$

$$\Rightarrow dU = TdS - pdV + \left(\frac{\partial G}{\partial m}\right)_{p,T} dm \quad (3.21)$$

Comparing Eq. (3.19) and (3.21), it is given as

$$\mu = \left(\frac{\partial G}{\partial m}\right)_{p,T} = \left(\frac{\partial U}{\partial m}\right)_{v,s} \quad (3.22)$$

Now, all quantities for unit mass of gas entering the chamber are taken,

$$\left(\frac{\partial G}{\partial m}\right)_{p,T} = \left(\frac{\partial H}{\partial m}\right)_{p,T} - \frac{\partial(TS)}{\partial m} \quad (3.23)$$

$$\Rightarrow \left(\frac{\partial G}{\partial m}\right)_{p,T} = h_c - T \frac{\partial S}{\partial m}$$

$$\Rightarrow h_c = \mu + Ts \quad (3.24)$$

This equation can be represented in Bond Graph.

3.3 THEORETICAL MODEL OF SHOCK ABSORBER

3.3.1 Energy equation for the upper chamber oil and lower chamber oil

It is noted that the oil does not enter and leave a chamber simultaneously, but sometimes enters and sometimes leaves the chamber according to the movement of the piston. So, sign speed

function is given as $f_1(t) = \frac{1 + \text{sign}[v(t)]}{2}$ and $f_2(t) = \frac{1 - \text{sign}[v(t)]}{2}$

where $sign[v(t)] = 1$ if $v(t) \geq 0$ and $sign[v(t)] = -1$ if $v(t) < 0$ and $v(t)$ is speed of shock absorber. Now, the general energy equation of upper chamber oil may be written as

$$\frac{d}{dt}[m.(i + KE + PE)]_{uc} = [\dot{m}(h + KE + PE)]_{in} - [\dot{m}(h + KE + PE)]_{out} + \dot{q}_{uc} - \dot{W}_{def-uc} \quad (3.25)$$

Within the boundaries of control volume, net flow-work is zero. So, internal energy is considered on the left side of the above equation. On the right side of above equation, enthalpy terms are considered because of the presence of flow work.

Potential energy and kinetic energy on the left side of Eq. (3.25) are neglected. Left side of Eq. (3.25) may be written as shown in Eq. (3.26).

$$\begin{aligned} & \frac{d}{dt}[m.i]_{uc} \\ & = d/dt[\rho.(A_p - A_r)L_{uc}(t)c_p.T_{uc}(t)] \\ & = \rho(A_p - A_r)L_{uc}(t)c_p\dot{T}_{uc}(t) + \rho(A_p - A_r)L_{uc}(t)c_p.T_{uc}(t) \end{aligned} \quad (3.26)$$

Now, considering the R.H.S of Eq. (3.25), total energy for the outlet and inlet flows is considered in the first and second term of Eq. (3.25). Sign function defined previously is used to take care of the flow of hydraulic fluid between the upper and lower chamber which depends on the direction in which piston is reciprocating inside the pressure tube. The properties of inlet flow to the upper chamber is considered to be same as the properties of the hydraulic fluid in the lower chamber and the properties of outlet flow from upper chamber are considered to be same as that of the properties of hydraulic fluid in the upper chamber. Potential and kinetic energies are considered as negligible and the equation can be written as

$$[\dot{m}.(h + KE + PE)]_{in} - [\dot{m}.(h + KE + PE)]_{out} = [\dot{m}.h]_{in} - [\dot{m}h]_{out} \quad (3.27)$$

As it is known that Enthalpy = Internal Energy + Flow Work. So, the above equation can be written as

$$\begin{aligned} [\dot{m}.i]_{in} - [\dot{m}.i]_{out} & = f_1[t]\rho.(A_p - A_r)\dot{L}_{uc}(t)\left[c_p.T_{uc}(t) + \frac{P_{uc}(t)}{\rho}\right] + \\ & f_2[t]\rho.(A_p - A_r)\dot{L}_{uc}(t)\left[c_p.T_{lc}(t) + \frac{P_{lc}(t)}{\rho}\right] \end{aligned} \quad (3.28)$$

In the equation 3.28, when the value of $v(t)$ is positive, the piston is moving upwards and sign $[v(t)]=1$, $f_1(t)=1$ and $f_2(t)=0$. Hence, the hydraulic fluid leaves the upper chamber. When the value of $v(t)$ is negative, the piston moves downwards and $f_1(t)=0$, $f_2(t)=1$. Hence, the hydraulic fluid enters into the upper chamber. Now, the heat transferred from the upper chamber hydraulic fluid to various parts of the shock absorber is given by the following equations.

1. Heat transfer from the upper chamber hydraulic fluid to the pressure tube.

$$(\dot{q}_{uc-pt}) = H_{uc-pt}(t) \cdot P_{int} L_{uc}(t) [T_{uc}(t) - T_{pt}(t)]$$

2. Heat transfer from the upper chamber hydraulic fluid to the piston.

$$(\dot{q}_{uc-p}) = H_{uc-p}(t) (A_p - A_r) [T_{uc}(t) - T_p(t)]$$

3. Heat transfer from the upper chamber hydraulic fluid to the piston rod.

$$(\dot{q}_{uc-pt}) = H_{uc-r}(t) \cdot P_{int,r} L_{uc}(t) [T_{uc}(t) - T_r(t)]$$

Now, the work term comprises of only the deformation work of the upper chamber hydraulic fluid which is given by multiplying the upper chamber pressure and volume deformation rate of the upper chamber hydraulic fluid.

$$\dot{W}_{def-uc}(t) = f_1 \cdot P_{uc}(t) (A_p - A_r) v(t) + f_2 P_{uc}(t) (A_p - A_r) v(t) \quad (3.29)$$

Now, substituting the various terms in the energy Eq. (3.25), the energy equation becomes

$$\begin{aligned} & -\rho (A_p - A_r) L_{uc}(t) c_p \dot{T}_{uc}(t) - \rho (A_p - A_r) L_{uc}(t) c_p T_{uc}(t) \\ & + f_1 [t] \rho (A_p - A_r) \dot{L}_{uc}(t) \left[c_p T_{uc}(t) + \frac{P_{uc}(t)}{\rho} \right] + f_2 [t] \rho (A_p - A_r) \dot{L}_{uc}(t) \left[c T_{lc}(t) + \frac{P_{lc}(t)}{\rho} \right] \\ & - H_{uc-pt}(t) \cdot P_{int} L_{uc}(t) [T_{uc}(t) - T_{pt}(t)] - H_{uc-pis}(t) (A_p - A_r) [T_{uc}(t) - T_{pis}(t)] \\ & - H_{uc-r}(t) \cdot P_{int,r} L_{uc}(t) [T_{uc}(t) - T_r(t)] + f_1 \cdot P_{uc}(t) (A_p - A_r) v(t) + f_2 P_{uc}(t) (A_p - A_r) v(t) = 0 \end{aligned} \quad (3.30)$$

The above equation contains the terms of temperature as dependent variable, time as independent variable and various pressure terms. But our aim is to derive a completely thermal model. So, the various pressure terms needs to be converted to some other form. For this, let us introduce the total energy equation of the flow inside the orifice of the piston connecting the rebound and the bump chamber.

$$\frac{d}{dt} [m.(i + KE + PE)]_{po} = [\dot{m}(h + KE + PE)]_{in} - [\dot{m}(h + KE + PE)]_{out} + \dot{q}_{po} - \dot{W}_{po} \quad (3.31)$$

Assumptions

- Inside the orifice, the unsteady effects are neglected.
- Energy transfer across the piston orifice boundary is neglected.
- The conditions of the hydraulic fluid at inlet are assumed to be of the upper chamber or lower chamber which depends on the direction of motion of piston.

The energy Eq. (3.31) can be written as

$$h_{in} = (h + KE)_{out} \quad (3.32)$$

For positive values of $v(t)$, the piston moves upwards inside the pressure tube and the upper chamber will act as inlet chamber and lower chamber will act as outlet chamber. So, the above equation takes the form as follows.

$$\begin{aligned} \left[c_p.T + \frac{P}{\rho} \right]_{uc} &= (c_p.T')_{u-1} + \left(\frac{P}{\rho_{oil}} \right)_{lc} + KE_{u-1} \\ \Rightarrow (c_p.T')_{u-1} - (c_p.T)_{u-1} &= \left(\frac{P}{\rho} \right)_{u-1} - \left(\frac{P}{\rho} \right)_{lc} - KE_{u-1} \end{aligned} \quad (3.33)$$

Here, $T' > T$. This is due to friction and irreversibilities while passing through the piston orifice. This heating effect is taken into account by introducing a term which is proportional to the kinetic energy of the hydraulic fluid flowing from upper chamber to the lower chamber.

$$(c_p.T')_{u-1} - (c_p.T)_{u-1} = K'.KE_{u-1}$$

$$\begin{aligned}
K'KE_{u-1} &= \left(\frac{P}{\rho}\right)_{uc} - \left(\frac{P}{\rho}\right)_{lc} - KE_{u-1} \\
\Rightarrow K'KE_{u-1} - KE_{u-1} &= \left(\frac{P}{\rho}\right)_{uc} - \left(\frac{P}{\rho_{oil}}\right)_{lc} \\
\Rightarrow (K'+1)(KE_{u-1}) &= \left(\frac{P}{\rho}\right)_{uc} - \left(\frac{P}{\rho_{oil}}\right)_{lc} \\
\Rightarrow K(KE_{u-1}) &= \left(\frac{P}{\rho}\right)_{uc} - \left(\frac{P}{\rho}\right)_{lc}
\end{aligned} \tag{3.34}$$

Where $K = K' + 1$. Both K and $K' + 1$ are constants.

$$\left(\frac{P}{\rho}\right)_{uc} = K(KE_{u-1}) + \left(\frac{P}{\rho}\right)_{lc} \tag{3.35}$$

Similarly, when the piston moves downwards, the lower chamber acts as inlet chamber and the upper chamber acts as outlet chamber.

$$\left(\frac{P}{\rho}\right)_{lc} = K(KE_{l-u}) + \left(\frac{P}{\rho}\right)_{uc} \tag{3.36}$$

Now, introducing the above two equation in the energy Eq. (3.25) of the upper chamber hydraulic fluid.

$$\begin{aligned}
& -\rho.(A_p - A_r)L_{uc}(t)c_p\dot{T}_{uc}(t) - \rho.(A_p - A_r)L_{uc}(t)c_p.T_{uc}(t) \\
& + f_1.\rho.(A_p - A_r)\dot{L}_{uc}(t)[c_p.T_{uc}] + f_1.\rho.(A_p - A_r)\dot{L}_{uc}(t)(K.KE_{u-1}) \\
& + f_1.\rho.(A_p - A_r)\dot{L}_{uc}(t)\left(\frac{P}{\rho}\right)_{lc} + f_2.\rho.(A_p - A_r)\dot{L}_{uc}(t)[c_p.T_{lc}] \\
& + f_2.\rho.(A_p - A_r)\dot{L}_{uc}(t)(K.KE_{l-u}) + f_2.\rho.(A_p - A_r)\dot{L}_{uc}(t)\left(\frac{P}{\rho}\right)_{uc} \\
& - H_{uc-pt}(t).P_{int}L_{uc}(t)[T_{uc}(t) - T_{pt}(t)] - H_{uc-pis}(t).(A_p - A_r)[T_{uc}(t) - T_{pis}(t)] \\
& - H_{uc-r}(t).P_{int,r}L_{uc}(t)[T_{uc}(t) - T_r(t)] + f_1.P_{uc}(t).(A_p - A_r)v(t) + f_2.P_{uc}(t).(A_p - A_r)v(t) = 0
\end{aligned}$$

Now, neglecting the density difference and introducing $\dot{L}_{up}(t) = -v(t)$

$$\begin{aligned}
& -\rho.(A_p - A_r)L_{uc}(t)c_p\dot{T}_{uc}(t) - \rho.(A_p - A_r)L_{uc}(t)c_p.T_{uc}(t) \\
& + f_1.\rho.(A_p - A_r)\dot{L}_{uc}(t)[c_p.T_{uc}] + Kf_1.\rho.(A_p - A_r)\dot{L}_{uc}(t)(KE_{u-1}) \\
& - f_1.(A_p - A_r)v(t).p_{lc} + f_2.\rho.(A_p - A_r)\dot{L}_{uc}(t)[c_p.T_{lc}] \\
& + Kf_2.\rho.(A_p - A_r)\dot{L}_{uc}(t)(KE_{1-u}) + f_2.(A_p - A_r)\dot{L}_{uc}(t).P_{uc} \\
& - H_{uc-pt}(t).P_{int}L_{uc}(t)[T_{uc}(t) - T_{pt}(t)] - H_{uc-pis}(t).(A_p - A_r)[T_{uc}(t) - T_{pis}(t)] \\
& - H_{uc-r}(t).P_{int,r}L_{uc}(t)[T_{uc}(t) - T_r(t)] + f_1.P_{uc}(t).(A_p - A_r)v(t) - f_2.P_{uc}(t).(A_p - A_r)\dot{L}_{uc}(t) = 0
\end{aligned}$$

$$\begin{aligned}
\Rightarrow & -\rho.(A_p - A_r)L_{uc}(t)c_p\dot{T}_{uc}(t) - \rho.(A_p - A_r)L_{uc}(t)c_p.T_{uc}(t) \\
& + f_1.\rho.(A_p - A_r)\dot{L}_{uc}(t)[c_p.T_{uc}] + Kf_1.\rho.(A_p - A_r)\dot{L}_{uc}(t)(KE_{u-1}) \\
& + f_2.\rho.(A_p - A_r)\dot{L}_{uc}(t)[c_p.T_{lc}] + Kf_2.\rho.(A_p - A_r)\dot{L}_{uc}(t)(KE_{1-u}) \\
& - H_{uc-pt}(t).P_{int}L_{uc}(t)[T_{uc}(t) - T_{pt}(t)] - H_{uc-pis}(t).(A_p - A_r)[T_{uc}(t) - T_{pis}(t)] \\
& - H_{uc-r}(t).P_{int,r}L_{uc}(t)[T_{uc}(t) - T_r(t)] + f_1.(P_{uc} - P_{lc}).(A_p - A_r)v(t) = 0
\end{aligned} \tag{3.37}$$

This is the required equation for the upper chamber hydraulic fluid. Proceeding in a similar manner, the equation for the energy equation for the lower chamber hydraulic fluid can be written as follows:

$$\begin{aligned}
& -\rho.(A_p)L_{lc}(t)c_p\dot{T}_{lc}(t) - \rho.(A_p)L_{lc}(t)c_p.T_{lc}(t) + f_1.\rho.(A_p)\dot{L}_{lc}(t)[c_p.T_{lc}] \\
& + Kf_1.\rho.(A_p)\dot{L}_{lc}(t)(KE_{(1-u)}) + f_2.\rho.(A_p)\dot{L}_{lc}(t)[c_p.T_{uc}] + Kf_2.\rho.(A_p)\dot{L}_{lc}(t)(KE_{(u-1)}) \\
& - H_{lc-pt}(t).P_{int}L_{lc}(t)[T_{lc}(t) - T_{pt}(t)] - H_{lc-p}(t).(A_p)[T_{lc}(t) - T_p(t)] \\
& + f_1.(P_{uc} - P_{lc}).(A_p)v(t) = 0
\end{aligned} \tag{3.38}$$

3.4 THERMAL MODEL FOR BOND GRAPH ANALYSIS

3.4.1 Basic Model of Shock Absorber

A general Bond Graph model for volume flow rates and pressure developed in the upper and lower chamber of hydraulic shock absorber can be obtained with the help of relationships used for volume flow rate and pressure.

The pressure development in the upper and lower chamber is a combination of two pressure terms. One is due to the movement of piston inside the pressure tube which leads to the continuous change in the volume of upper and lower chamber which further lead to the pressure change and its intensity is same in all directions. Hence, it is known as isotropic pressure. It is given by stress-strain equation incorporating the bulk modulus as given in Eq. (3.39).

$$\Delta P = -\beta \left(\frac{\Delta V_c}{V_c} \right) \quad (3.39)$$

where ΔV_c is the change in volume, V_c is initial volume, β is Bulk modulus of elasticity.

Other term for the pressure is due to compressibility of the hydraulic fluid in motion and this is called anisotropic pressure. Consider an infinitesimal element of fluid. Total stress acting on this fluid element is given by Eq. (3.40).

$$\sigma_{ij} = \mu \left(\frac{\partial u_i}{\partial x_j} + \frac{\partial u_j}{\partial x_i} \right) + \mu_1 \delta_{ij} \nabla \cdot u \quad (3.40)$$

where μ = dynamic viscosity, μ_1 = second viscosity coefficient, δ_{ij} = Kronecker delta, u = velocity vector.

In Eq. (3.40), the first term on the right hand side represents the stress due to shape change and it is known as deviatoric stress. The second term on the right side of equation represents the stress due to volume change and it is known as hydrostatic stress. Kronecker delta is used to take into account only the normal stresses.

Now, the viscous force per unit volume in direction of x_i can be obtained by differentiating the Eq. (3.40) with respect to the rectangular coordinate x_j .

$$\frac{F_i}{V} = \frac{\partial}{\partial x_j} \left[\mu \left(\frac{\partial u_i}{\partial x_j} + \frac{\partial u_j}{\partial x_i} \right) + \mu_1 \delta_{ij} \nabla \cdot u \right] \quad (3.41)$$

For flow in direction of piston movement only, $\nabla \cdot u = \frac{\partial \dot{V}}{\partial V}$. Here $\frac{\partial \dot{V}}{\partial V}$ is volumetric strain.

Neglecting shear stress, Eq. (3.41) can be written as follows:

$$\sigma_{xx} = \mu_1 \frac{\partial \dot{V}}{\partial V} \quad (3.42)$$

Now, the pressure will develop in the upper and lower chamber of the shock absorber due to this stress and the magnitude of this pressure will be equal to the stress but acts in direction opposite to the stress. For the Newtonian fluid, the Eq. (3.42) can be written as

$$P_a = -\mu_1 \left(\frac{\dot{V}_c}{V_c} \right) \quad (3.43)$$

where P_a is anisotropic pressure developed, \dot{V}_c is volume flow rate of hydraulic fluid and V_c is volume of upper or lower chamber. Subscript c stands for upper or lower chamber.

Eqs. (3.39) and (3.43) represent the pressure development in the upper and lower chamber of the shock absorber. These two equations are represented in the bond graph to calculate the pressure development. Two R-elements are used as dampers with a damping constant of $\frac{\mu_1}{V_c}$ to represent the Eq. (3.43). In this way anisotropic pressure in the two chambers is calculated. Further two C-fields are used to represent Eq. (3.39) and hence the pressure due to compressive force of piston is calculated by taking capacitance coefficient equal to $\frac{\beta}{V_c}$. The basic bond graph model for pressure and volume flow rates is shown in Fig. 3.20.

The volume flow rate of hydraulic fluid passing through the piston orifice is a function of pressure difference occurring between the two sides of the piston. Bernoulli's equation can be applied to calculate the volume flow rate through the piston orifice.

$$\Delta P = P_{uc} - P_{lc} = \frac{1}{2} \rho v_{lc}^2 - \frac{1}{2} \rho v_{uc}^2 \quad (3.44)$$

Now, the sign of ΔP decides the direction of flow of hydraulic fluid *i.e* whether the flow takes place from upper chamber to lower chamber or from lower chamber to upper chamber. So the function sign ΔP have to be included in the formula. Hence the Eq. (3.44) can be written as

$$\Delta P = \left(\frac{1}{2} \rho v_{lc}^2 - \frac{1}{2} \rho v_{uc}^2 \right) \times \text{sign}(\Delta P) \quad (3.45)$$

Using continuity equation, the sectional areas and volumetric flow rates can be substituted for the velocity terms. So the Eq. (3.45) can be written as

$$\Delta P = \frac{1}{2} \rho Q^2 \frac{1}{A_{lc}^2} \left(1 - \frac{A_{lc}^2}{A_{uc}^2} \right) \times \text{sign}(\Delta P) \quad (3.46)$$

$$\Rightarrow \dot{Q} = \sqrt{\frac{2\Delta P}{\rho}} \frac{A_{lc}}{\sqrt{1 - \frac{A_{lc}^2}{A_{uc}^2}}} \quad (3.47)$$

This equation is applicable to the ideal flow conditions only. So, in order to account for the frictional effects, viscosity of fluid and turbulence, real flow situation needs to be considered. So, the Eq. (3.47) can be reduced to the real flow equation by introducing the coefficient of discharge. The value of coefficient of discharge is obtained experimentally and it lies between 0.6-0.9. Also the area term is replaced by simply A_v (area of piston orifice). The final equation for the volumetric flow rate can be written as

$$\dot{Q} = C_d A_v \sqrt{\frac{2\Delta P}{\rho}} \quad (3.48)$$

Now, this equation is used in bond graph to calculate the volumetric flow rate of hydraulic fluid. This equation takes into account only the volume flow rate due to the isotropic pressure difference occurring because of movement of piston. Volumetric strain is not considered in this relation. Taking into account the volumetric strain, the two R-fields are used to calculate the volumetric flow rates for the upper and lower chamber. Basic bond graph model for the Twin-tube shock absorber is shown in Fig. 3.20.

Input force (Se) applied is given by $F_{\text{damp}} \sin \omega t$. This force is measured by applying detector on the energy port. I-element on the junction-1_p represents the mass of piston. For measuring the piston displacement, flow detector is placed which measures the velocity of piston which is further integrated to find the piston displacement. Next comes the two transformer elements which converts the input force to pressure developed in the upper and lower chamber by simply dividing the input force with $A_p - A_r$ for the upper chamber and by A_p for the lower chamber. At the 1-junctions, two R-elements (one for upper chamber and other for lower chamber) are used as dampers with a damping constant of $\frac{\mu_1}{V_c}$ to represent the Eq. (3.43). In this way anisotropic pressure in the two chambers is calculated. Further two C-fields are used to represent Eq. (3.39) and hence the pressure due to compressive force of piston is calculated by taking capacitance coefficient equal to $\frac{\beta}{V_c}$. Junction-0_{uc} receives this effort (which is total pressure developed in the upper chamber) from the 1-junction on the left side and flow detector is placed on the port to calculate this effort. Similarly, 0_{lc}-junction receives total pressure developed in the lower chamber as effort from the junction-1 on the right side and flow detector is placed on the port to measure the pressure developed in the lower chamber.

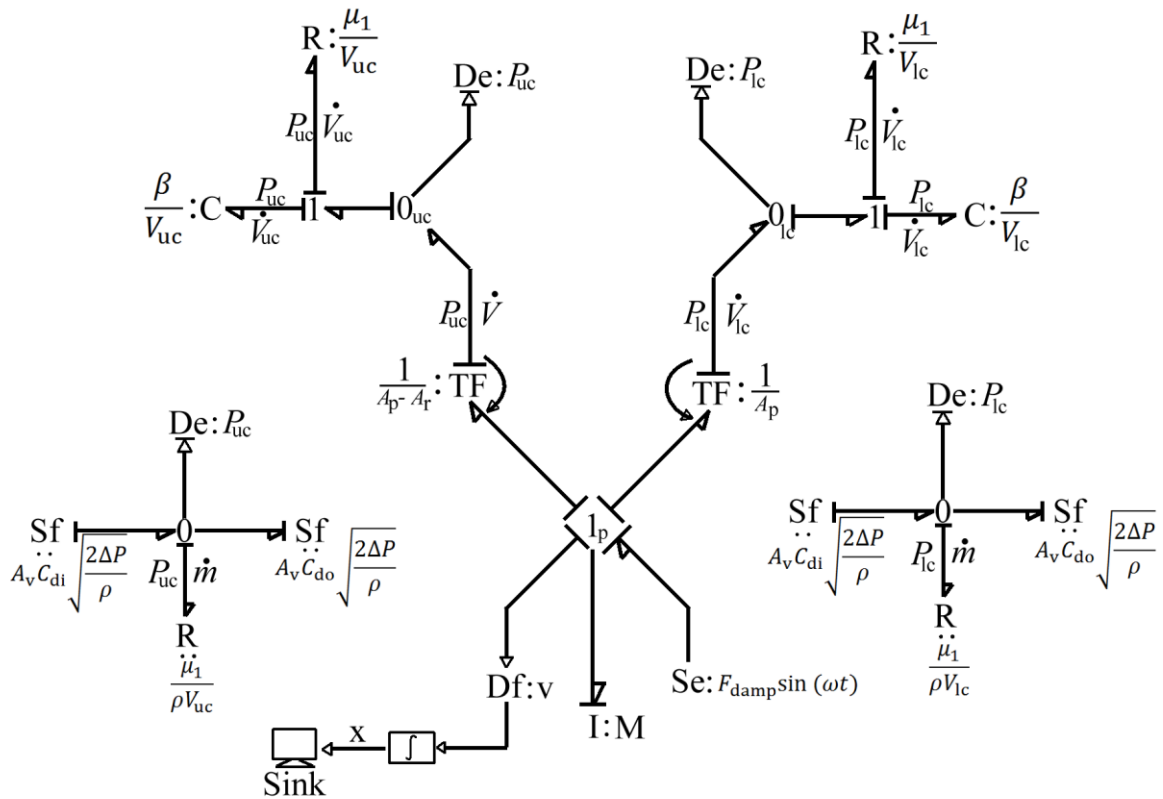


Fig. 3.20 Basic Bond Graph Model for Shock Absorber

Two 0-junctions are used to calculate the volume flow rate of hydraulic fluid in the upper chamber and lower chamber. Flow of hydraulic fluid between the upper and lower chamber is due to the pressure difference between the two chambers. Taking into account the volumetric strain, the two R-fields are used to calculate the volumetric flow rates for the upper and lower chamber.

3.4.2 Thermal Model

Thermal model is developed by considering the enthalpy flow as a function of mass flow rate of hydraulic fluid. Model for the mechanical part remains same as discussed above. The only difference is the inclusion of thermal C-field. Two C-fields are used to calculate the temperature of upper and lower chamber. Enthalpy, which is a function of mass flow rate of hydraulic fluid, acts as source of flow. C-element takes in flow as input enthalpy and gives out effort as a temperature. Input enthalpy is taken at ambient temperature and it is given by Eq. (3.49).

$$h = \dot{m} c_p T_{ambient} \quad (3.49)$$

Thermal model is similar to the basic model shown in fig. 3.20, with an only difference of inclusion of two C-fields for calculating the temperature development in the upper and lower chamber. Mass flow rate calculated in the basic model for shock absorber is taken in the enthalpy equation. In other words, enthalpy is taken as the function of mass flow rate of hydraulic fluid through the piston. At the 0-junction on the top left side, initial enthalpy is taken as source of flow. C element on the left side receives this enthalpy as flow and returns a temperature as effort. In this way, the temperature development in the upper chamber is measured. Similarly, the 0-junction at the top right side calculates the temperature in the lower chamber. Further the R-element is used to take care of the temperature rise with time which results in enthalpy rise. The output of the R-element is added to the initial enthalpy. So, the enthalpy term is updated every time as the temperature rises. Thermal Bond Graph model for the hydraulic shock absorber is shown in Fig. 3.21.

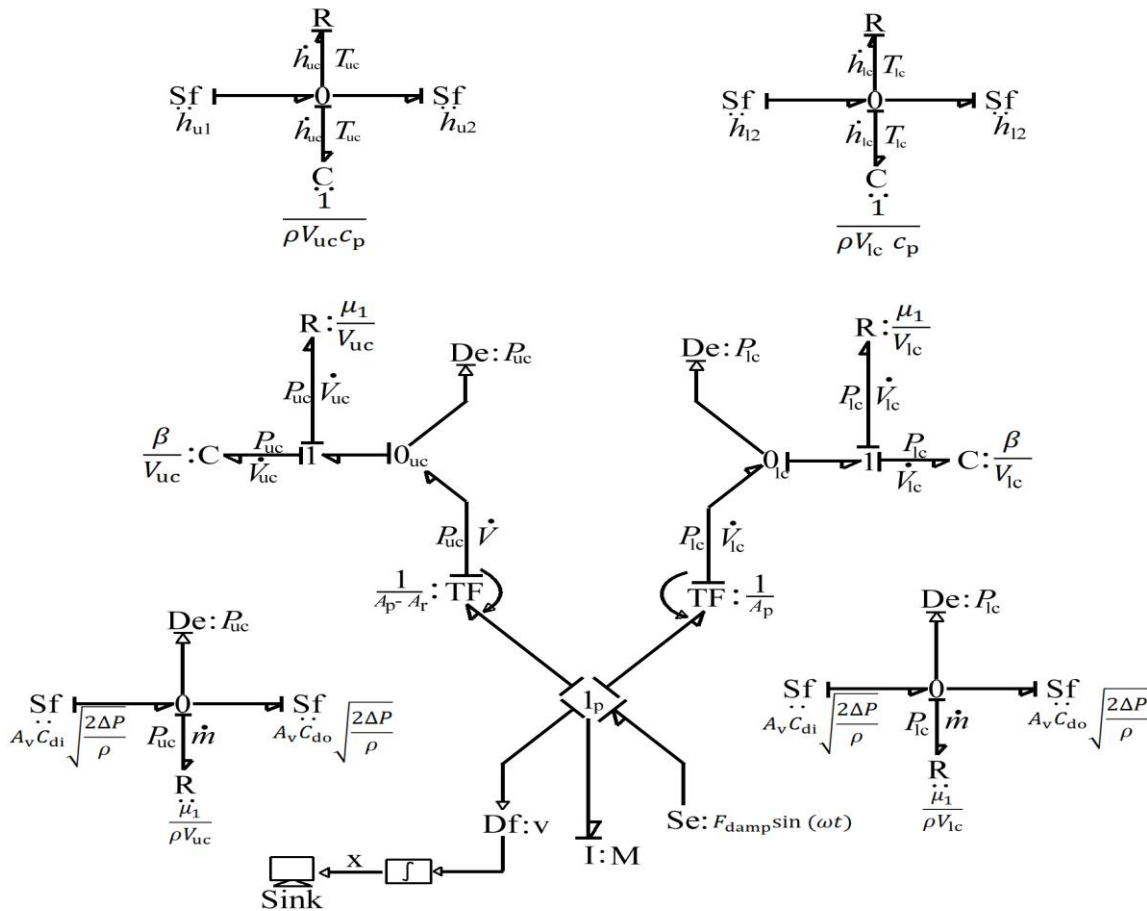


Fig. 3.21 Thermal bond graph model for twin-tube shock absorber

3.4.3 Thermal Model with heat losses

The thermal model described above evaluates the temperature of hydraulic fluid. In order to evaluate the surface temperature of the shock absorber, material properties of shock absorber are taken into account. It is assumed that the heat is flowing outwards in the radial direction. As the temperature is raising with time, so the whole interval is broken up into small sub-intervals. Heat generated for these sub intervals is calculated using the Eq. (3.50)

$$q = \dot{m}c_p T_{\text{final}} - T_{\text{initial}} \quad (3.50)$$

The calculated heat generated is equated to the heat going out of the system by conduction and convection. Eq. (3.51) gives the temperature of the surface of shock absorber.

$$q = \frac{T_{\text{oil}} - T_{\text{surface}}}{\frac{1}{h_{\text{oil}}A_{r_1}} + \frac{\ln\left(\frac{r_2}{r_1}\right)}{2\pi kL} + \frac{1}{h_{\text{oil}}A_{r_2}} + \frac{1}{h_{\text{oil}}A_{r_3}} + \frac{\ln\left(\frac{r_4}{r_3}\right)}{2\pi kL}} \quad (3.51)$$

From Eq. (3.41) temperature at the surface of shock absorber is found as we know the temperature of oil. Convective and conductive resistances accounts for the heat loss.

3.5 PARAMETER VALUES AND SIMULATION RESULTS

Table 3.3: Parameter values for the hydraulic and thermal model of twin-tube shock absorber

Parameter	Value
L	0.24m
R _p	0.01246m
R _r	0.0062m
β	3.7*10 ⁵ N/m ²
ρ	970 kg/m ³
m _p	0.05kg
F _{damp} at 1" stroke length	35N
F _{damp} at 2" stroke length	70.7N
F _{damp} at 3" stroke length	120N
F _{damp} at 4" stroke length	170N

P_{in}	$1*10^5 \text{N/m}^2$
A_v	0.00001m^2
ω	3.66rad/s
C_{di}	0.60
C_{do}	0.60
μ_1	1.3
c_p	$2250 \text{Jkg}^{-1}\text{K}^{-1}$
f_{uc}	0.2
f_{ic}	0.1

3.5.1 Variation of Input Force with Time

Input force is given in the form of sine wave which is approximately same as the nature of input force applied in the experiment. In Fig. 3.22, it is shown that input force for compression stroke is negative and it is positive for rebound stroke. Simulation results of input force are shown for 10 seconds at different stroke length of piston.

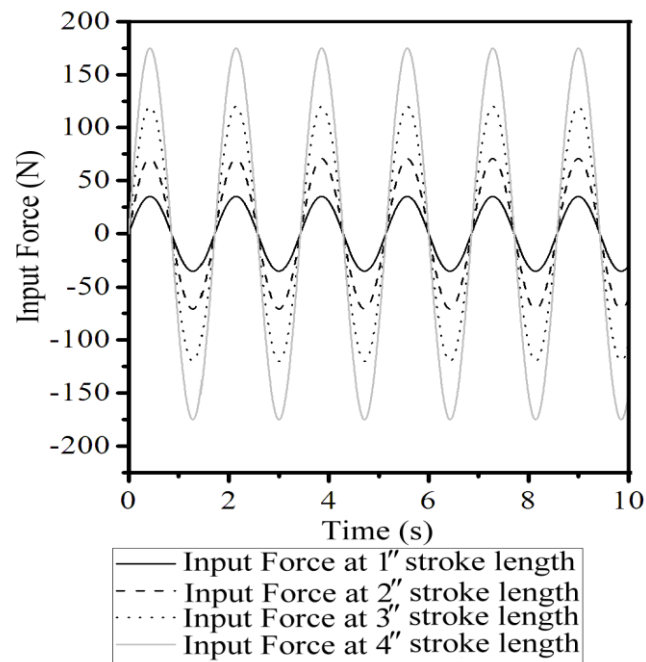


Fig. 3.22 Variation of Input Force with Time

From the Fig. 3.22, it is seen that the input force increases with increase in the stroke length of piston for the same frequency of 35 Hertz.

3.5.2 Variation of Piston Displacement with Time

Middle position of piston is taken as reference. Now, the piston displacement at different stroke length is plotted against time.

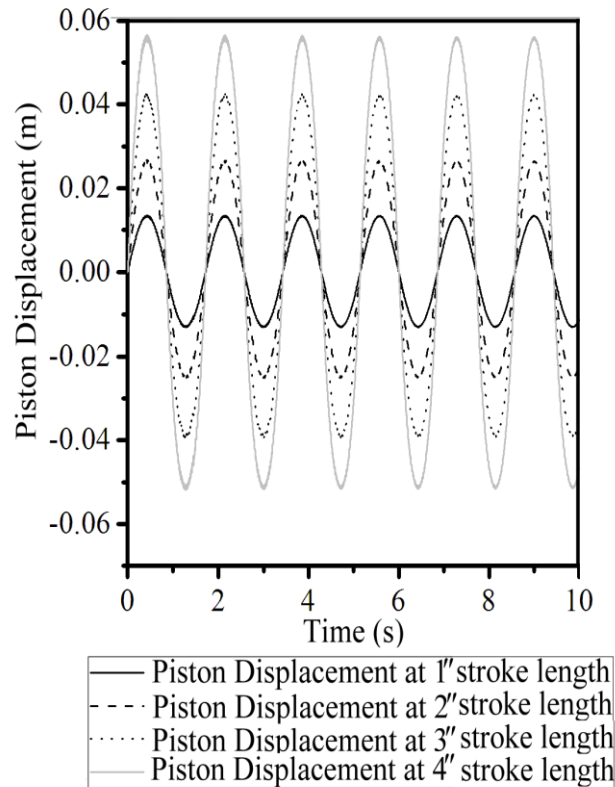


Fig. 3.23 Variation of Piston Displacement with Time

Piston displacement is the major factor upon which depend the many features of shock absorber like pressure development, volume flow rate of oil, temperature development. Thus the major performance characteristics of piston depend mainly on the piston displacement. In Fig. 3.23, variation of piston displacement at different stroke lengths is shown. Piston displacement is maximum for maximum stroke length of the piston. In the subsequent results, it is shown that the pressure, volume flow rate and temperature of oil increases with increase in stroke length of the piston. Hence, it is concluded that higher is the piston displacement, higher will be the pressure

and temperature developed in the upper chamber and lower chamber of the shock absorber. Also, there will be increased volume flow rate of oil with increased values of piston displacement.

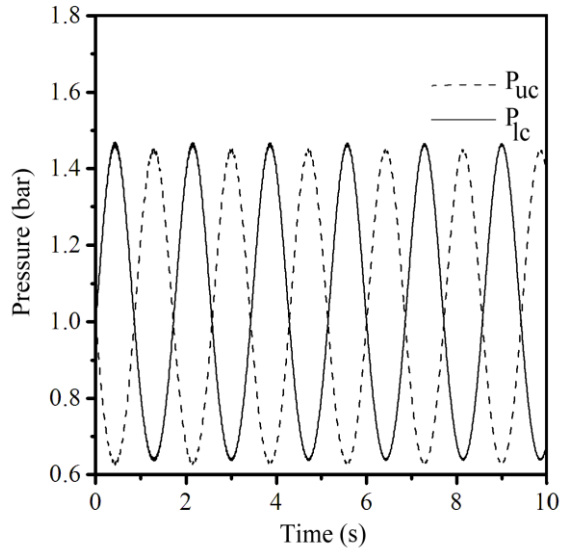
3.5.3 Variation of Pressure Developed in Upper and Lower Chamber at different stroke lengths with Time

As the piston reciprocates inside the shock absorber, there will be changes in the pressure in the upper and lower chamber according to the direction of motion of the piston that is whether it is moving upward or downward. During the compression stroke, the piston moves downward, so there is increase in the pressure in the lower chamber as the piston advances downward. At the same time, there is some loss of pressure in the lower chamber due to oil flowing out of this chamber into the upper chamber and reserve chamber through the piston orifice and base valve respectively. But the loss of pressure in the lower chamber due to mass going out of this chamber is negligible as compared to rise in pressure due to high compression force. Also, as the oil passes through the piston orifice, there will be conversion of pressure of pressure energy into kinetic energy. So, the increase in pressure of the upper chamber due to mass flow into this chamber during the compression is negligible. Further, there is loss of pressure in the upper chamber during the compression stroke due to increase in volume of this chamber.

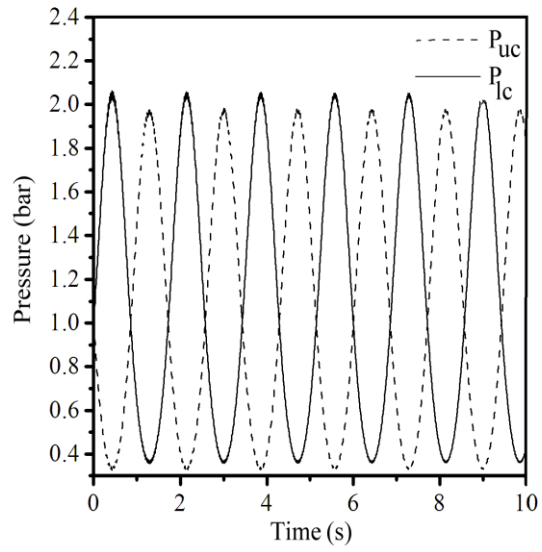
During the rebound stroke, the piston moves upward, so there is increase in the pressure of upper chamber as the piston advances upward. Furthermore, there is some loss of pressure in the upper chamber due to oil flowing out of this chamber into the lower chamber through the piston orifice. But this loss of pressure of the upper chamber is negligible as compared to rise in pressure due to high rebound force. Also, there is conversion of pressure energy into kinetic energy as the oil passes through the piston orifice. Moreover, there are friction losses in the piston orifice. So the pressure rise of lower chamber due to mass flow into this chamber during the rebound stroke is also negligible. Due to the increase in volume of lower chamber during the rebound stroke, there is loss of pressure in this chamber during the rebound stroke.

The Fig. 3.24 shows that the pressure rise is increased as the stroke length of piston is increased. This is obvious, as the stroke length of piston increases, there is high compressive and rebound forces which lead to the development of high pressure with increase in stroke length of the piston. Curve for the pressure variation in upper chamber and lower chamber is plotted against time for the piston stroke length of 1", 2", 3" and 4". This differential Pressure

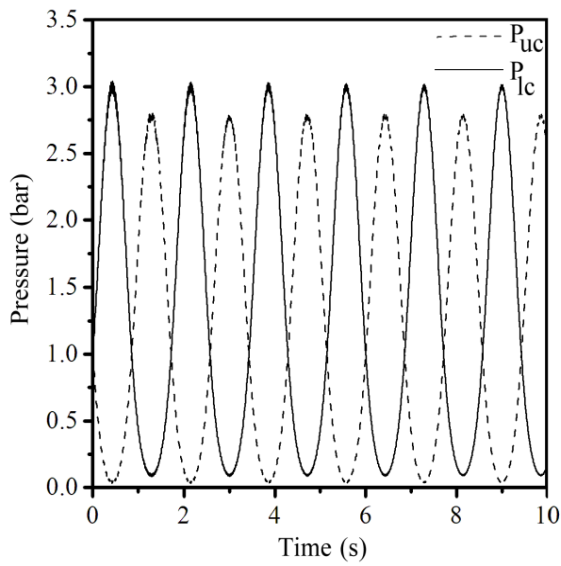
development in the upper and lower chamber is the driving force for the flow of oil between the two chambers through the piston orifice.



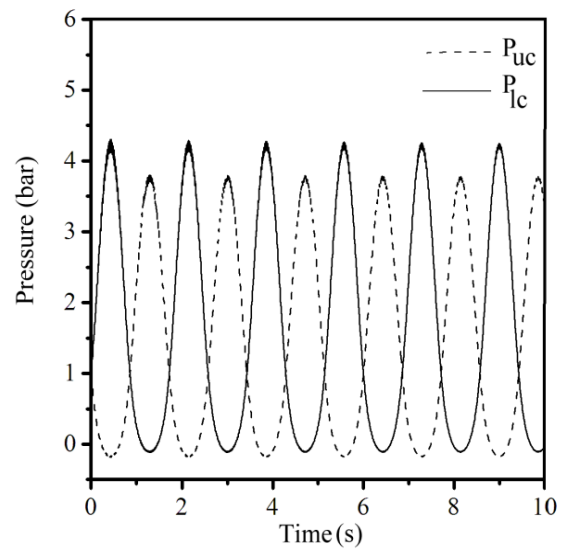
(a)



(b)



(c)



(d)

Fig. 3.24 Variation of Pressure Developed in Upper and Lower Chamber at (a) 1" stroke length, (b) 2" stroke length, (c) 3" stroke length and (d) 4" stroke length

3.5.4 Volume flow rate for the Upper chamber and Lower chamber

The volume flow rate of oil passing through the piston orifice is a function of pressure difference occurring between the two sides of the piston. Oil passing through the piston orifice experiences a pressure drop across the orifice. This pressure drop is used to calculate the volume flow rate of oil through the piston orifice. Bernoulli's equation for incompressible flow is applied to calculate the volumetric flow rate of oil.

During the compression stroke, the piston moves downward. As a result of which, there exists a pressure difference between the upper chamber and lower chamber. There is development of high pressure in the lower chamber and low pressure in the upper chamber. Now, this pressure difference acts as effort for the volumetric flow of oil from the lower chamber to upper chamber. So, during the compression stroke, there is flow of oil from lower chamber to upper chamber.

Now during the rebound stroke, the piston moves upward. So, there will be development of high pressure in upper chamber and low pressure in lower chamber. Now, this pressure difference acts as driving effort for the flow of oil from lower chamber to upper chamber. In a nutshell, there is flow of oil from upper chamber to lower chamber during the rebound stroke.

Further, the damping capacity of shock absorber depends upon the resistance offered by the piston orifice to the flow of oil through it. It is always advantageous to have comparatively large flow rate during the compression stroke than during the rebound stroke in order to achieve smooth rebound action of shock absorber. So, to achieve this, piston orifice should be designed in such a way that it offers less resistance to the flow of oil during the compression stroke as compared to rebound stroke.

In Fig. 3.25 and Fig 3.26, it is seen that the volume flow rate through the piston orifice increases as the stroke length of piston increases. It is observed that the flow rate of oil from lower chamber to upper chamber during the compression stroke is slightly more than the flow rate of oil from upper chamber to lower chamber during the rebound stroke. Further, the difference between the volume flow rate of oil between the upper chamber and lower chamber increases as the stroke length of piston increases. It means piston orifice provides more resistance to the flow of oil from upper chamber to lower chamber as compared to the flow of oil from lower chamber to upper chamber. Thus, the shock absorber provides better damping force during the rebound stroke which leads to the smooth rebound action of shock absorber. This is

the most desirable performance characteristic of the shock absorber which depends mainly on the geometrical configuration of the piston orifice.

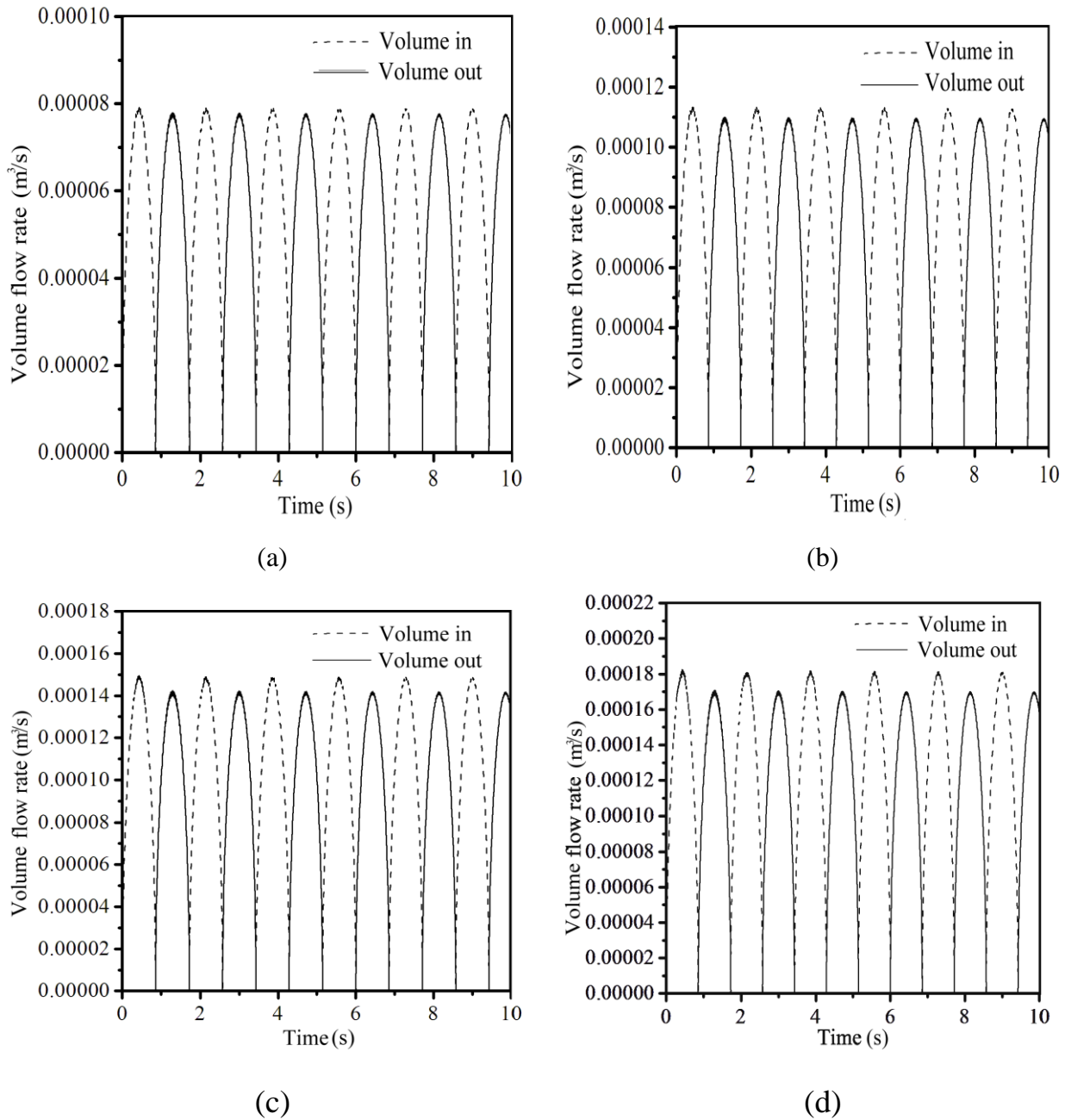
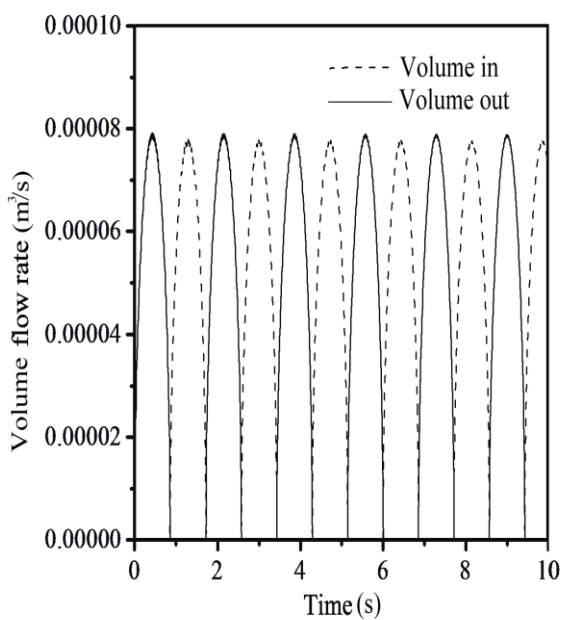
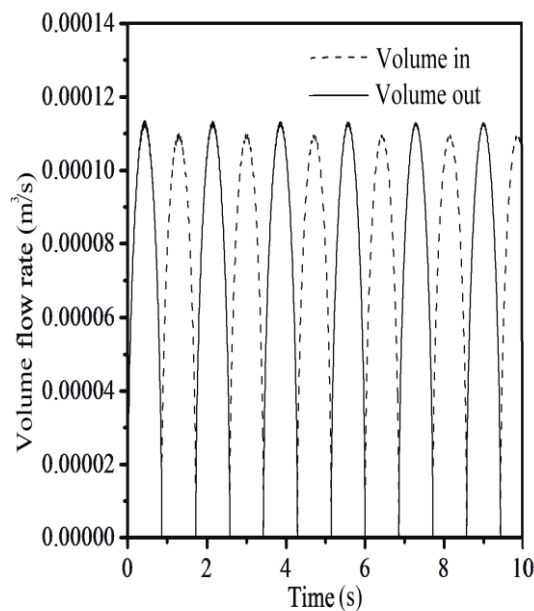


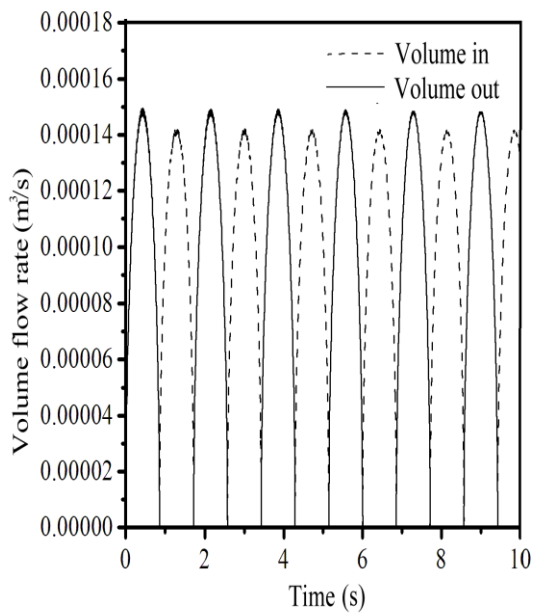
Fig. 3.25 Volume flow into and out of upper chamber of shock absorber at (a) 1" stroke length, (b) 2" stroke length, (c) 3" stroke length and (d) 4" stroke length



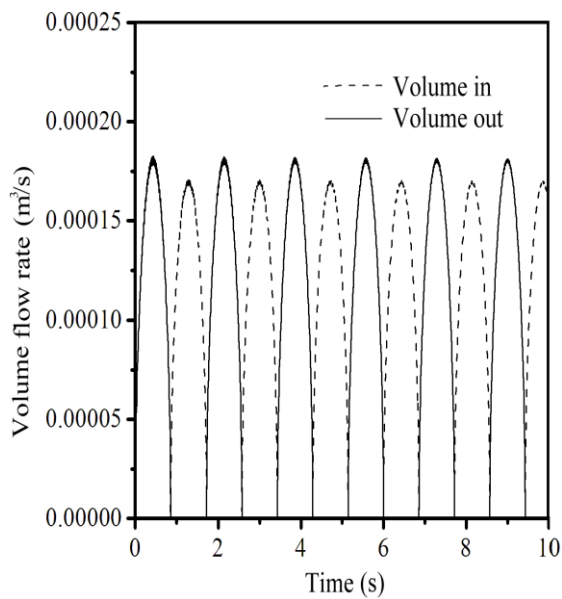
(a)



(b)



(c)



(d)

Fig. 3.26 Volume flow into and out of lower chamber of shock absorber at (a) 1" stroke length, (b) 2" stroke length, (c) 3" stroke length and (d) 4" stroke length

In Fig. 3.25, it is seen that oil flows into upper chamber during the compression stroke and out of the upper chamber during the rebound stroke. Variation of volume flow into and out of upper chamber with time is shown. In Fig. 3.26, simulation result for the variation of volumetric flow of oil into and out of the lower chamber is shown. It is seen that the oil flows into lower chamber during the rebound stroke and out of the lower chamber during the compression stroke.

3.5.5 Variation of Oil Temperature for Upper chamber and Lower chamber with Time

As already described in the working of shock absorber, there is conversion of kinetic energy (given to the shock absorber by the external excitation) to heat energy when the shock absorber provides damping effect to the vibrations caused due to external excitation. So, there is temperature rise of oil inside the shock absorber due to accumulation of heat. This heat needs to be dissipated to the atmosphere so as not to ill effect the performance of the shock absorber.

In Fig. 3.27, the variation of oil temperature of upper chamber and lower chamber with time is shown. Temperature rise in the upper chamber is comparatively more due to high mass flow rate of oil in the upper chamber during the compression stroke as compared to the mass flow rate of oil in the lower chamber during the rebound stroke. And it is seen that the temperature difference between upper chamber and lower chamber is increasing with increase in the stroke length of the piston. The reason for this increasing temperature differential with increase in the piston stroke length between the upper chamber and lower chamber is that with increase in stroke length of piston, difference between the mass flow rates of oil through piston orifice increases. Thus, the temperature difference between the upper chamber and lower chamber for 1" stroke length is lowest and that for 4" stroke length is highest. It is also seen from the Fig. 8 that the temperature saturates after some time. The saturation of temperature is achieved after about 35 minutes when the piston stroke length is 1" or 2". The saturation of temperature in case of 3" and 4" stroke length of piston is achieved after about 40 minutes. It means the saturation point is achieved faster in the case of smaller stroke lengths of piston as compared to the larger stroke lengths of the piston. Also the heat transfer to the surrounding is unsteady till the attainment of saturation state of temperature. After the saturation point is achieved, the heat transfer to the surrounding becomes steady. And this is the maximum heat

transfer rate which is achieved after the saturation point. Temperature profiles of upper chamber and lower chamber at stroke length of 1", 2", 3" and 4" are shown below.

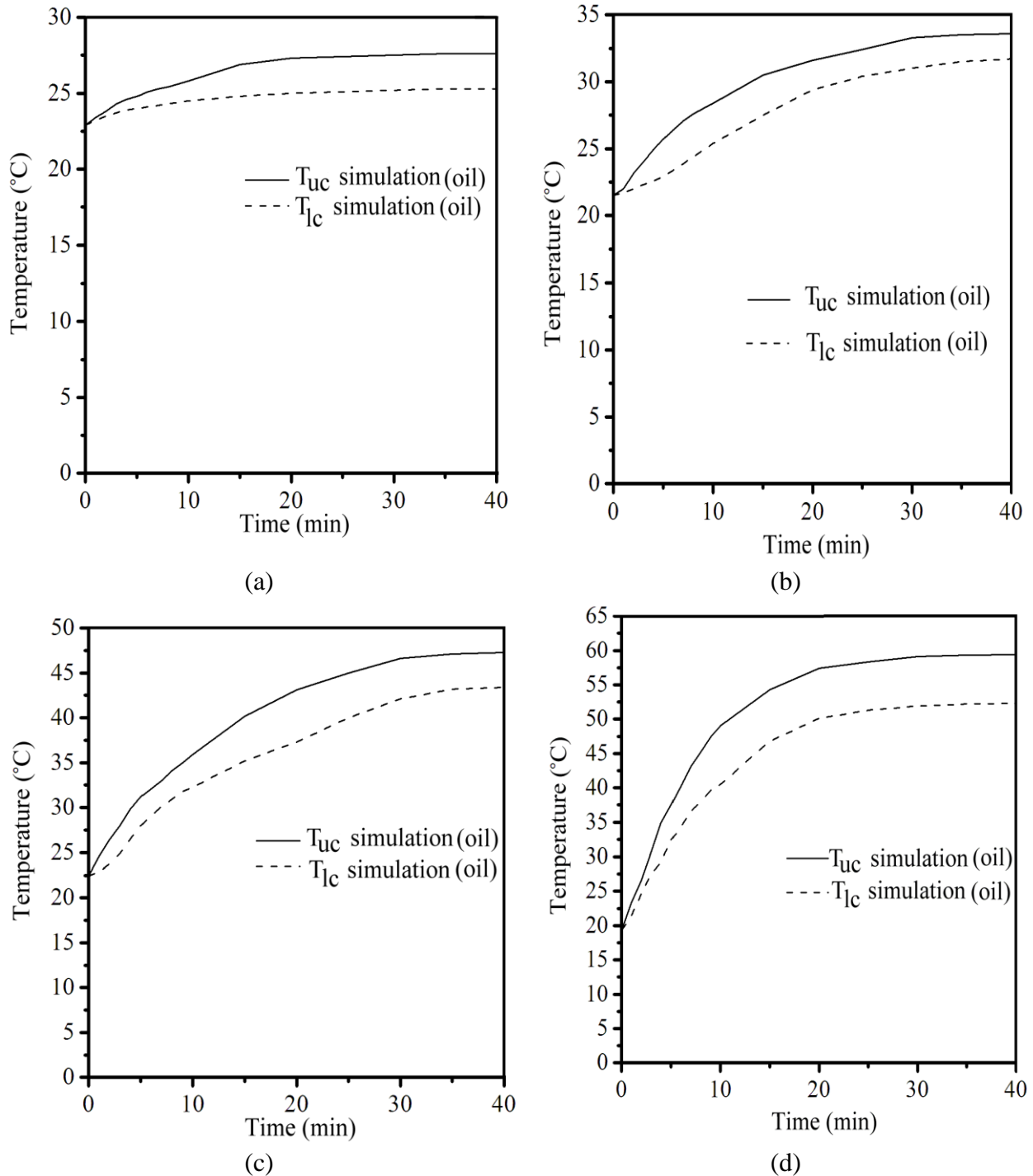


Fig. 3.27 Variation of Oil Temperature for Upper chamber and Lower chamber at (a) 1" stroke length, (b) 2" stroke length, (c) 3" stroke length and (d) 4" stroke length

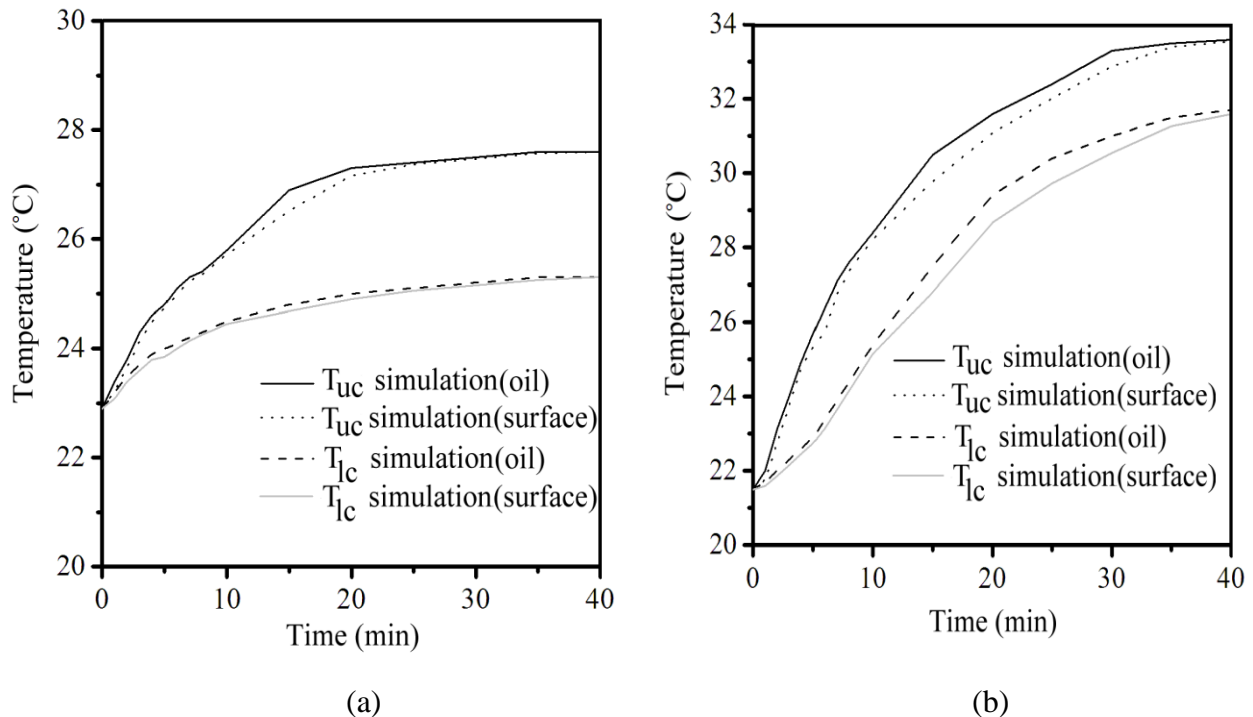
3.5.6 Comparison between Oil Temperature and surface temperature for Upper chamber and Lower chamber

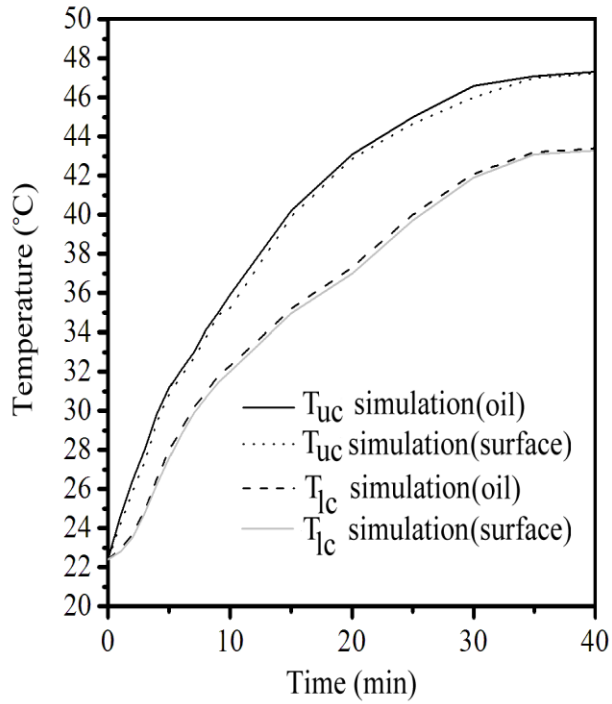
The phenomenon of temperature development in the shock absorber is quite simple. As the piston starts reciprocating inside the cylinder due to external excitation, the temperature of oil starts to rise because of enthalpy flow between the upper chamber and lower chamber given by

$$\dot{h} = \dot{m} c_p \Delta T$$

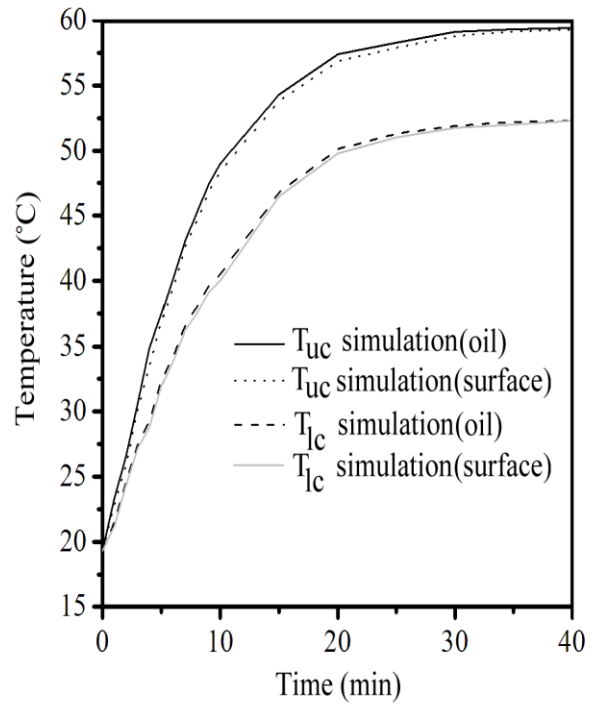
Further, this enthalpy flow is dependent on the mass flow rate of oil through the orifice. Because of this dependence of enthalpy flow on the mass flow rate of oil, temperature of oil in upper chamber is comparatively higher than temperature of oil in the lower chamber. Initially, when the piston just starts reciprocating, the outside surface temperature of shock absorber is lower than the oil temperature for both chambers. After some time, there will be a saturation of temperature of oil. Also at this point, the temperature of oil becomes equal to the surface temperature of shock absorber. It is at this point that the maximum heat transfer to the surroundings starts to occur and the system achieves equilibrium. The heat transfer after this point becomes steady state problem.

In Fig. 3.28, Variation of oil temperature and shock absorber surface temperature for upper chamber and lower chamber is shown. It is observed that oil temperature and outside surface temperature of shock absorber become equal after about 40 minutes.





(c)



(d)

Fig. 3.28 Comparison between the Oil Temperature and surface temperature for Upper chamber and Lower chamber at (a) 1" stroke length, (b) 2" stroke length, (c) 3" stroke length and (d) 4" stroke length

4.1 INTRODUCTION

Description of various components used in the experiment and comparison of simulation results with the experimental results is presented in this chapter. Experimental set up consists of the slotting machine, twin-tube shock absorber, piezoelectric dynamometer, k-type thermocouple, multichannel charge amplifier for force measurement. Slotting machine is used to give input external force to the twin-tube shock absorber and dynamometer is used to measure this sinusoidal force. Temperature rise of hydraulic fluid in the upper and lower chamber of shock absorber is measured with the help of k-type thermocouple with display screen.

4.2 EXPERIMENTAL SETUP

The various components included in the experimental setup are slotting machine, twin-tube shock absorber, piezoelectric dynamometer and k-type thermometer as shown in Fig. 4.1. First of all, components are installed in a way to measure the temperature rise of upper and lower part of the twin-tube shock absorber. Three-jaw chuck is fastened to the bed of the slotting machine. Three-jaw chuck holds the bottom end of the shock absorber, the piston-rod end of the shock absorber being fastened to the reciprocating ram of the slotting machine. The stroke length of the piston can be adjusted by fixing the initial position of the shock absorber.



Fig. 4.1 Twin-Tube shock absorber fixed on the slotting machine for temperature measurement

As the slotting machine is started, the piston of shock absorber starts to reciprocate in the pressure tube of shock absorber. The temperature of hydraulic fluid in the shock absorber starts to rise. Now, the temperature has been measured by fixing the thermocouple to the upper and lower part of the shock absorber. Temperature has been measured for different stroke lengths of the piston. Fig. 4.1 shows the shock absorber being fixed on the slotting machine and thermocouples are attached to it.

Input force measurement has been done after the measurement of temperature. Three jaw chuck has been replaced by the piezoelectric dynamometer for the measurement of force. Dynamometer has been fastened to the bed of the slotting machine. Then the bottom end of twin-tube shock absorber is fastened to the upper plate of the dynamometer by the nut and bolt, the rod end of shock absorber being fixed to the reciprocating ram of the slotting machine. As the machine is started, the piston starts to reciprocate inside the pressure tube of the shock absorber. The input force of the slotting machine makes an impact on the sensor of the dynamometer, which in turn deforms and generates voltage as output. This output voltage is calibrated in terms of force to give the direct reading of force. Input force is measured for the different stroke lengths of the piston. Twin-Tube shock absorber fixed on a dynamometer for force measurement is shown in Fig. 4.2.



Fig. 4.2 Twin-Tube shock absorber fixed on a dynamometer for force measurement

4.2.1 Four-Component Dynamometer (Type 9272)

Piezoelectric dynamometer is used for the measurement of the input force given to the shock absorber. It is four-component dynamometer that can measure the force in all the three perpendicular directions (i.e x-component, y-component and z-component) along with torque. The dynamometer is made up of highly rigid material and has a very high natural frequency. Its resolution is very high which makes it possible to measure even the smallest dynamical changes in force and torque. It is basically used to measure the cutting forces in the universal drilling machine. The piezoelectric dynamometer fitted to the bed of slotting machine is shown in Fig. 4.3.



Fig. 4.3 Four-Component Dynamometer (Type 9272)

The dynamometer consists of base plate and top plate. There is a four component sensor which is fitted with a high preload between these plates. All the four components can be measured without any displacements. It is to be noted that there are chances of reduction in the range that can be measured by the dynamometer due to presence of eccentric and combined loads. In order to eliminate the problems of ground loop and vibrations, the sensor is mounted in such a way that it is ground-isolated. The material of dynamometer is rust-proof and a special protection is provided against the cooling agents and the splash water penetration into the sensors. Protection class level of IP 67 is achieved by providing high level protection to the dynamometer.

In the present work, piezoelectric dynamometer is fitted to the bed of the slotting machine. The bottom end of the twin-tube shock absorber is fastened to the dynamometer

through the nut and bolt. Piston-rod end of shock absorber is fastened to the reciprocating ram of the slotting machine.

4.2.2 Multichannel Charge Amplifier for Multi component Force Measurement

Multichannel Charge Amplifier is an instrument used along with piezoelectric dynamometer. Its function is to convert the mechanical deformation of piezoelectric sensor into the equivalent voltage output. Electric charge is produced when force exerts a pressure on the piezoelectric sensor plate. The produced electrical charge is directly proportional to the pressure which acts on the piezoelectric sensor. This electrical charge is converted into the proportional voltage by the charge amplifier. The charge amplifier is further connected to the computer system which has Kistler software installed in it. The voltage signal is converted into proportional force output by the software. Multi charge Amplifier is shown in Fig. 4.4.



Fig. 4.4 Multi charge Amplifier

4.2.3 K-Type Thermocouple with Display Unit

K-type wire thermocouples with display are used to measure the temperature of the upper and lower part of the twin-tube shock absorber. Various grades and types of thermocouple wire are available in the market. In the wire type thermocouple, there are two types of wires used. One is thermocouple grade wire which acts as a probe element for the temperature measurement and other is extension grade wire which is connected to probe element at one end and to display unit

at other end. Material used for the thermocouple grade wire is metal alloys of specific combination. Usually a wire of nickel-alumel alloy is welded to a nickel-chromium alloy wire. It is not only the combination of alloys which are used but also the purity of alloys, on which the wire grade depends. Thermocouple grade wire is more expensive, high grade and highly accurate as compared to the extension grade wire because the main function of temperature measurement is performed by the thermocouple grade wire and the function of extension grade wire is just to connect the thermocouple wire to the display unit.

Two K-type wire thermocouples with display unit are used in the experiment. One thermocouple is attached at the upper part of the shock absorber and other at the lower part of shock absorber. Adhesive tape is used to attach the thermocouples with the shock absorber. The other end of the thermocouples is connected the display unit. Temperature readings have been taken directly from the display unit at regular intervals of time. Temperature measured by one thermocouple can be displayed on the display unit at a time. So, Toggle switch is used to change the temperature of thermocouple being displayed. Fig. 4.5 shows the thermocouples attached to the shock absorber.



Fig. 4.5 K-type Wire Thermocouple with Display Unit

4.2.4 Twin-Tube Shock Absorber

Rear Shock Absorber of Tata Innova is test for the thermal stability. It is gas filled hydraulic shock absorber of Twin-tube type. It consists of two cylinders called outer cylinder or reserve tube and inner cylinder or pressure tube. Material of the pressure tube and reserve tube of twin-tube shock absorber is mild steel. Maximum stroke length of the piston is 6". Temperature in the upper and lower part of shock absorber is measured for the piston stroke length of 1", 2", 3" and 4". Input force is also measured for the same stroke lengths. The dimensions of various parts of Twin-tube shock absorber are given in Table 4.1.

Table 4.1: Shock Absorber Dimensions

Sr no.	Part	Dimension
1	Outside diameter of outer cylinder	44.92mm
2	Inside diameter of outer cylinder	43.74mm
3	Thickness of outer cylinder	1.18mm
4	Outside diameter of inner cylinder	27.08mm
5	Inside diameter of inner cylinder	25.90mm
6	Thickness of inner cylinder	1.18mm
7	Piston diameter	24.92mm
8	Rod diameter	12.40mm
9	Length of inner cylinder	240mm
10	Length of outer cylinder	260mm
11	Length of piston rod	180mm

For the temperature measurement, bottom end of the shock absorber is fixed in the three jaw chuck which is fastened to the bed of the slotting machine and rod end of the shock absorber is fastened to the ram of the slotting machine. For the input force measurement, the bottom end of shock absorber is fastened to the plate of dynamometer which is fixed on the bed of the slotting machine, rod end of the shock absorber being fixed to the ram of the slotting machine as in case of temperature measurement.

4.2.5 Slotting Machine

Slotting machine with a maximum stroke length of 12 inch is used. Primary function of slotting machine is cutting slots, but here it is utilized to give input force to the shock absorber which makes the piston the shock absorber to reciprocate inside the pressure tube. The experiment is conducted for different stroke lengths of the piston. The stroke is adjusted by setting the stroke adjustment lever. Experiment is conducted at the stroke length of 1", 2", 3" and 4". Slotting machine used in the experiment is shown in Fig. 4.6.

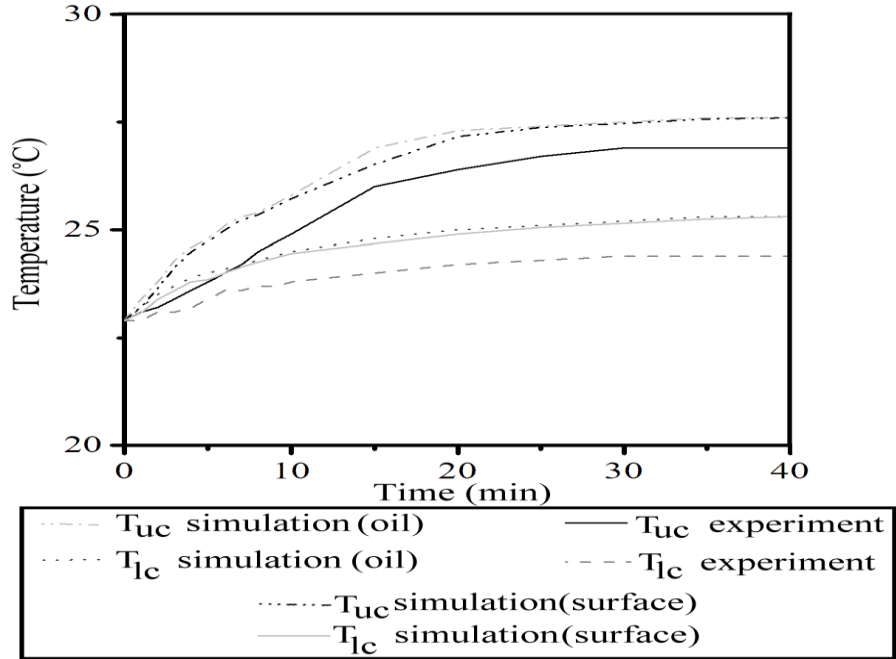


Fig. 4.6 Slotting Machine

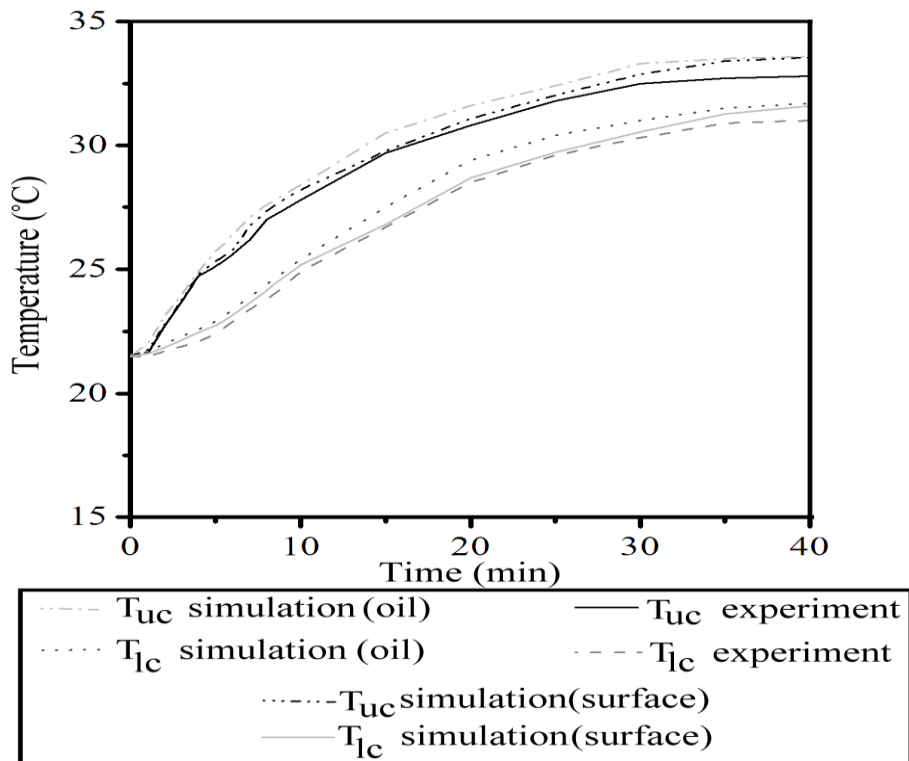
4.3 COMPARISON OF SIMULATION AND EXPERIMENTAL TEMPERATURE PROFILES

When the input force is given to the rod of the shock absorber, the piston starts to reciprocate inside the pressure tube. Enthalpy rise in the upper and lower chamber of shock absorber is taken as function of mass flow rate of hydraulic fluid through the piston orifice. So, the temperature of hydraulic fluid starts to rise when input force is given. Temperature is measured for the upper and lower part of shock absorber by attaching k-type thermocouples at the surface. Temperature is measured for the piston stroke length of 1", 2", 3" and 4". It is found that the temperature becomes constant after about 35 minutes for piston stroke length of 1" and 2" and it is becoming constant after approximately 40 minutes for the piston stroke length of 3" and 4". This point is known as saturation point. The reason for this saturation is that the temperature difference between the surface of shock absorber and hydraulic fluid becomes zero. Heat transfer become maximum after this point.

Simulation is done for temperature development by considering the enthalpy rise of the hydraulic fluid as function of volume flow rate of fluid through the piston orifice. Simulation and experimental results vary to a very small extent. Temperature in the simulated results is slightly greater than the experimentally measured temperature, the difference being 0.1 to 0.7 °C for the entire time interval at all the stroke lengths of piston. The reason for this difference is that there are various assumptions in the simulated model. The conductive heat loss to the slotting machine through the clamping is not considered. Radiation loss is not considered. Temperature profiles for the simulated and experimental results are shown in Fig. 4.7.



(a)



(b)

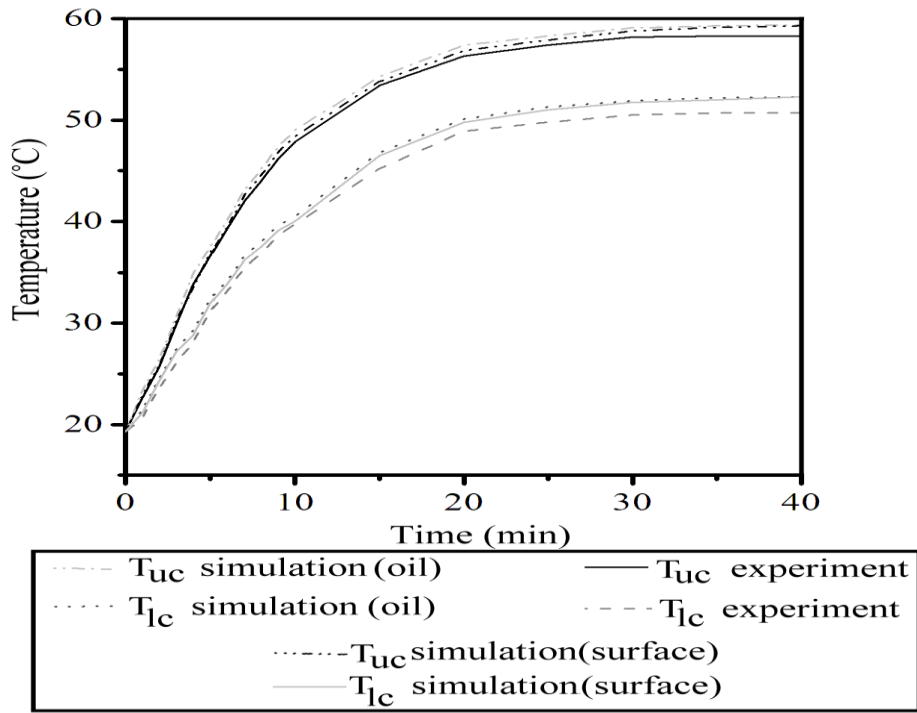
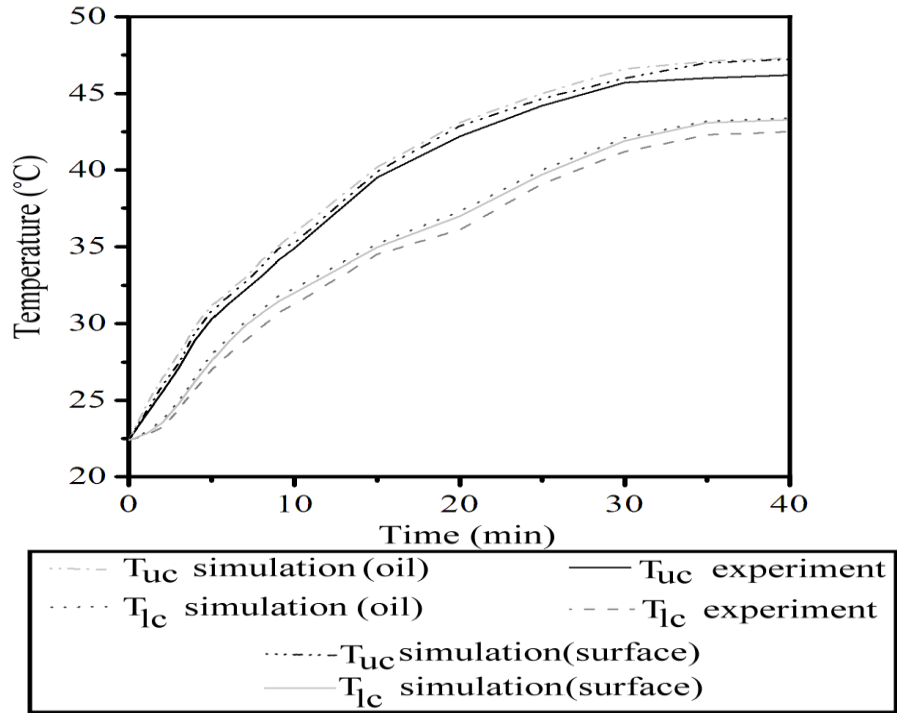


Fig. 4.7 Variation of Temperature for the experimental and simulation results at (a) 1" stroke length, (b) 2" stroke length, (c) 3" stroke length and (d) 4" stroke length

5.1 CONCLUSION

The objective of this Thesis was to develop a thermal model for the twin-tube hydraulic shock absorber using bond graph method. Simulation results are compared with the experimental results to validate the model. The conclusions made from this Thesis work are given below:

- Both the experimental and simulation results show that the volume flow rate of hydraulic fluid is more in the upper chamber as compared to that in the lower chamber. This is due to the geometrical configuration of piston orifice which allows high volume flow rate of hydraulic fluid during the downward or compression stroke and comparatively low volume flow rate during the upward or rebound stroke. This is the reason for the smooth and comfort that we feel after the vehicle hits an obstruction. Volume flow rate increases with increase in the stroke length of piston.
- Pressure development in the upper and lower chamber is a combination of two pressure terms *i.e.*, isotropic pressure due to volume change of upper and lower chamber when the piston reciprocates and anisotropic pressure due to the compressibility of fluid. The pressure differential between the upper chamber and lower chamber acts as the driving force for the flow of hydraulic fluid. Graph for the pressure development follows a sine wave. Pressure in both the chambers increases with increase in the stroke length of the piston.
- Temperature of hydraulic fluid in the upper and lower chamber is modeled by taking enthalpy as flow variable in the bond graph. Temperature in the upper chamber is comparatively higher than the temperature in the lower chamber. This is due to the higher volume flow rate of hydraulic fluid into the upper chamber as compared to that in the lower chamber. Temperature rises linearly with respect to time for about 35 minutes in case of stroke length of 1" and 2" and for about 40 minutes in case of stroke length of 3" and 4". There is a saturation of temperature after this point. At this point, the surface temperature and hydraulic fluid temperature become equal and shock acts as a single entity transferring heat to the surroundings. This point marks the point of maximum heat transfer to the surroundings.

- The bond graph model developed in this thesis work may be used by the manufacturers to know the hydraulic and thermal performance of their product. Further, it will help the manufacturers in deciding the size and number of piston orifices which is deciding factor for the comfort level of the vehicle.

5.2 SCOPE FOR FUTURE WORK

Based on this thesis, the following areas of work are suggested for further investigation:

- Bond graph model with varying material properties of shock absorber may be developed so as to select the material for which the maximum heat transfer takes place.
- Geometrical configuration of piston orifice and optimum number of piston orifices required to achieve the comfort level at disturbances of different magnitude may be investigated.
- Thermal bond graph model for different hydraulic fluids may be developed so as to select the fluid with maximum heat transfer to the surroundings.

REFERENCES

- [1] Hassan, S. A., Thesis on fundamentals studies of passive, active and semi active automotive suspension system, 1986.
- [2] Reimpell, J., Stoll, H., and Betzler, J., The automotive Chassis, *Engineering Principles*, Second Edition, **34**, 2001, 73–85.
- [3] Margolis, D. L., and Shim, T., A bond graph model incorporating sensors, actuators and vehicle dynamics for developing controllers for vehicle safety, *Journal of the Franklin Institute*, **338**, 2001, 21–34.
- [4] Dauphin-Tanguy, G., Rahmani, A., and Sueur, C., Bond graph aided design of controlled systems, *Simulation Practice and Theory*, **7** (5–6), 1999, 493–513.
- [5] Gawthrop, P. J., Physical model-based control: A bond graph approach, *Journal of the Franklin Institute*, **332** (3), 1995, 285–305.
- [6] Karnopp, D. C., Margolis, D. L., and Rosenberg, R. C., *System Dynamics, Modelling and Simulation of Mechatronic Systems*, 2000 (John Wiley & Sons, NY).
- [7] Borutzky, W., *Bond Graphs-A Methodology for Modelling Multidisciplinary Dynamic Systems*, 2004 (SCS Publishing House, Erlangen, San Diego).
- [8] Mukherjee, A., Karmakar, R., and Samantaray, A. K., *Bond Graph in Modelling, Simulation and fault Identification*, 2006 (CRC Press, FL).
- [9] Samantaray, A. K., and Ould Bouamama, B., *Model-based Process Supervision*, 2008 (Springer Verlag, London).
- [10] Aridhi, E., Abbes, M., and Mami, A., Pseudo Bond graph Model of a Thermo-Hydraulic System, *LACCS Laboratory of Analyze, Conception and Control of Systems*, **2092**.
- [11] Brown, F.T., Bond Graph based simulation of thermodynamic models, *Journal of Dynamic systems, measurement and Control*, **132**, 2010, 064501(1)-064501(3)
- [12] Calvo, A.J., Caldas, C.A., and Roman, J.L., Analysis of Dynamic Systems Using Bond Graph Method through Simulink, *Engineering Education and Research Using MATLAB*, 2011.

- [13] Ramos J. C., Rivas A., Biera J., Sacramento G. and Sala J. A., Development of thermal model for automotive twin-tube shock absorber, *Applied Thermal Engineering*, **25**, 2005, 1836–1853.
- [14] Ferdec U., LUCZKO J., Modeling and Analysis of a Twin Tube Hydraulic Shock Absorber, *Journal of Theoretical and Applied Mechanics*, **50** (2), 2012, 627–638.
- [15] Lee C. T., Moon B.Y., Simulation and experimental validation of vehicle dynamic characteristics for displacement-sensitive shock absorber using fluid-flow modeling, *Mechanical Systems and Signal Processing*, **20**, 2006, 373–388.
- [16] Rathod P.P., Sorathiya A.S. and Patel D.R., Heat Transfer Study of Damping Fluid and improvement of Air-gap in shock absorber operation, *International Journal of Engineering Research & Technology*, **1** (3), 2012.
- [17] Xiaobing N., Jisheng S. and Laiqian W., Modeling and experiment of vehicle double-tube hydraulic shock absorber, *Electric Information and Control Engineering (ICEICE)*, 2011, 2334–2337.
- [18] Dong P., Shuang X.P. and Wang W.R., Modeling and Prediction of Vehicle Tube Hydraulic Shock Absorbers Based on BP Neural Network, *Machine Learning and Cybernetics*, 2006, 2935–2939.
- [19] Titurus B., Bois J.D., Lieven N. and Hansford R., A method for the identification of hydraulic damper characteristics from steady velocity inputs, *Mechanical systems and signal processing*, **24**, 2010, 2868–2887.
- [20] Ferreira C., Ventura P., Morais R., Valente A.L.G., Neves C. and Reis M.C., Sensing methodologies to determine automotive damper condition under vehicle normal operation, *Sensors and Actuators A: Physical*, **156**, 2009, 237–244.
- [21] Goldasz J., Modeling of Amplitude Selective Damping Valves, *Mechanics and Control*, **30** (2), 2011, 60–64.
- [22] Satpute, N.V., Singh, S., and Sawant, S.M., Fluid Flow Modelling Of A Fluid Damper With Shim Loaded Relief Valve, *International Journal of Mechanical Engineering (IJME)*, **2** (1), 2013, 65–74.
- [23] Simms, A., and Crolla, D., The Influence of Damper Properties on Vehicle Dynamic Behaviour, *World Congress Detroit*, 2002.

- [24] Comas, A., and Alonso, M., Thermal model of a twin-tube cavitating shock absorber, Proceedings of the Institution of Mechanical Engineers, *Part D: Journal of Automobile Engineering*, 2002.
- [25] Lion, A., and Loose, S., A Thermomechanically Coupled Model for Automotive Shock Absorbers: Theory, Experiments and Vehicle Simulations on Test Tracks, *Vehicle System Dynamics: International Journal of Vehicle Mechanics and Mobility*, **37** (4), 2002, 241–261.
- [26] Witter, M., and Swevers, J., Black-box model identification for a continuously variable, electro-hydraulic semi-active damper, *Mechanical Systems and Signal Processing*, **24**, 2010, 4–18
- [27] Spelta, C., Savaresi, S., and Fabbri, L., Experimental analysis of a motorcycle semi-active rear suspension, *Control Engineering Practice*, **18**, 2010, 1239–1250.
- [28] Vassal, C. P., Savaresi, S. M., Spelta, C., Sename, O., and Dugard, L., A Methodology for Optimal Semi-Active Suspension Systems Performance Evaluation, *49th IEEE Conference on Decision and Control (CDC 2010), Atlanta, Georgie : United States*, 2010.
- [29] Mori, T., Nilkhamhang, I. and Sano, A., Adaptive semi active control of suspension system with MR damper, System Design Engineering, keio university yokohama, japan, 223–8522.
- [30] Ping, H., Wang, Y., Zhang, Y., Liu, Y., and Xu, Y., Integrated control of semi-active suspension and vehicle dynamics control system, *International Conference on Computer Application and System Modelling (ICCASM)*, 2010.
- [31] Hassan, S. A., Thesis on fundamentals studies of passive, active and semi active automotive suspension system, 1986.

CURRICULUM VITAE

Amritveer Singh did his graduation from Baba Banda Singh Bahadur Engineering College in Bachelor of Mechanical Engineering (B. Tech), in the year 2012. In the same year, he joined the Master of Engineering (Thermal Engineering) Programme at Thapar University, Patiala, Punjab through GATE-2012. His ME thesis work is in the area of Development of a Thermal Model for a Twin-Tube Shock Absorber: Experimental and Modeling Approach. One journal paper from his research work is under preparation. Presently, he is working as a Junior Engineer in Water Supply and Sanitation Department (Government of Punjab).